

A lightweight low-power magnetometer-based
UAV flight control system
ELEC 480

Matthew J. Chave

November 3, 2005

Abstract

An autonomous flying robot was designed, built and tested which uses magnetometers as the source of attitude information. The complete control system was designed and built, including the electronics and the software required for a first order autonomous flight. The flight controller is capable of being installed on many airframes. It was successfully tested on a small electric-powered model aircraft controlling both heading and pitch.

Acknowledgements

This project could not have been successful if it was not for all of the following people.

Firstly, to Tim Molteno my supervisor, Tim without your enthusiastic input (including your fixed point math library which you whipped up just as it was needed), this project could have never succeeded. To all the electronics research people, particularly: Jared Laverty, Patrick Suggate, Phil Brown, Tom Mulder, Paul Williams, Hilary Lawrence, and Simon Harvey. You all must be thanked for each of your valuable input. Thank you also to Alan Coppard for making your time available to test fly the aircraft. To everyone who made this year simple so that I could concentrate on this project.

Finally, to the Canham family, your friendship and generous support throughout my studies is something which leaves me completely lost for words. This work is dedicated to you.

Thank You All.

Contents

| | | |
|----------|---|-----------|
| 1 | Introduction | 8 |
| 1.1 | Overview | 10 |
| 2 | Design Considerations | 12 |
| 2.1 | Sensors | 12 |
| 2.1.1 | Attitude | 13 |
| 2.1.2 | Inertial State | 14 |
| 2.1.3 | Coordinated control | 15 |
| 2.1.4 | Airspeed | 16 |
| 2.1.5 | Position Measurement | 17 |
| 2.1.6 | Battery health and current consumption | 17 |
| 2.2 | Support Hardware | 18 |
| 2.2.1 | Analog input | 18 |
| 2.2.2 | Mode selection UAV/RPV | 19 |
| 2.2.3 | (De)Multiplexing the controller to servo output | 19 |
| 2.3 | The processor | 22 |
| 3 | PCB Design and Layout | 23 |
| 3.1 | Main Board | 23 |
| 3.2 | Sensors | 23 |
| 3.2.1 | Triaxial magnetometer | 23 |
| 4 | Magnetometer Attitude Determination | 26 |
| 4.1 | Local reference magnetic field calculation | 26 |
| 4.2 | Body referenced magnetic field given desired attitude | 28 |
| 4.3 | Calculating rotation to achieve desired attitude | 30 |
| 5 | Flight Control System | 32 |
| 5.1 | Sensor measurement | 32 |
| 5.1.1 | Conditioning | 32 |
| 5.1.2 | Sampling | 35 |

| | | |
|----------|---|-----------|
| 5.1.3 | Calibration | 35 |
| 5.2 | Attitude detection | 36 |
| 5.3 | Output | 36 |
| 5.3.1 | Servo output | 37 |
| 5.3.2 | Telemetry/Debugging output | 37 |
| 5.3.3 | SPI communication for ADC and miscellaneous on-board packages | 37 |
| 5.4 | Simple first approach | 37 |
| 5.4.1 | PID control | 38 |
| 5.4.2 | Attitude Control | 40 |
| 5.4.3 | Simple turn | 40 |
| 5.5 | Navigation | 40 |
| 5.5.1 | Measuring the current location | 41 |
| 5.5.2 | Waypoints | 41 |
| 5.5.3 | Achieving way points | 41 |
| 5.5.4 | Calculating required attitude to the next waypoint | 41 |
| 5.5.5 | Course corrections, adjusting for environmental effects | 41 |
| 5.6 | Flight dynamics | 42 |
| 5.6.1 | Roll | 42 |
| 6 | Airframe | 46 |
| 7 | Test Flight Results | 49 |
| 7.1 | Goals | 49 |
| 7.2 | Method | 50 |
| 7.3 | Trimming, Balancing and calibrating the airframe | 51 |
| 7.4 | Select a location | 51 |
| 7.5 | Results | 53 |
| 8 | Conclusions | 58 |
| 8.1 | Further work | 59 |
| 8.1.1 | Coping with noise and inaccuracy | 59 |
| 8.1.2 | Number representation | 59 |
| 8.1.3 | Further development | 59 |
| A | Quaternions | 61 |
| A.1 | Multiplying quaternion numbers | 62 |
| B | Significant code | 64 |
| B.1 | Reference field rotation | 64 |
| B.2 | Map measured field to reference field | 64 |

| | | |
|-----|---|----|
| B.3 | Rotation from measured to reference magnetic field for attitude | 65 |
| B.4 | Proportional control | 65 |
| B.5 | Navigation | 65 |

List of Tables

| | | |
|-----|---|----|
| 2.1 | Trimble Lassen SQ parameters (from [8]) | 18 |
| 6.1 | GWS E-Starter airframe specifications | 47 |
| 7.1 | Magnetic field information near Dunedin | 52 |

List of Figures

| | | |
|-----|--|----|
| 1.1 | The GWS E-Starter airframe | 10 |
| 2.1 | Hardware block diagram for UAV | 12 |
| 2.2 | Sensors from left to right: GPS antenna, GPS module, magnetometers and pressure sensor, accelerometers, Gyros. | 13 |
| 2.3 | Rotations about the magnetic field vector produce the same readings [6] | 14 |
| 2.4 | Aircraft inclinometer [14] | 16 |
| 2.5 | UAV/RPV switch | 20 |
| 2.6 | Timing Diagram for the Johnson counter from [16] | 21 |
| 3.1 | Fully assembled main board, the 40 pin connectors are for the ARM module | 24 |
| 3.2 | Eagle Board design picture | 24 |
| 3.3 | 3 axis magnetic field board design layout, measuring 5cm by 2cm | 25 |
| 3.4 | 3 axis magnetic field sensor board | 25 |
| 4.1 | World map of the magnetic declination as of 2005, in degrees with contour interval of 2 degrees [12] | 28 |
| 5.1 | Implementation of the control system | 33 |
| 5.2 | Second order low pass butterworth filter | 33 |
| 5.3 | Spice simulated filter, red represents amplitude, blue phase, with frequency horizontal. | 34 |
| 5.4 | Non-Inverting amplifier schematic | 35 |
| 5.5 | Wind can be calculated as the difference between heading and bearing | 42 |
| 6.1 | The control system installed onto the E-Starter | 48 |
| 7.1 | The ground station setup for updating the firmware, offsets, and gains in the field | 54 |

7.2 A series of still images from video footage showing the transition from pilot control to autonomous control. The frames read from left to right, top to bottom. They are taken at regular intervals every 18 frames which represents approximately 0.71s depicting a controlled turn toward north. 57

Chapter 1

Introduction

Unmanned Air Vehicles (UAV) control systems appear to have begun development primarily for military purposes only a few years after the first manned flight of 1903. UAV technology began to take shape driven by the first world war when in 1917 the Sperry Aerial Torpedo developed in the USA used a gyroscopic stabilizer to fly 50 miles [1], becoming the first UAV by flying via remote control.

The reliance on radio control was removed a year later in 1918 with the Kettering Aerial Torpedo. Invented by Charles F. Kettering, developed for the U.S. military and built by Dayton-Wright Airplane Company, the aircraft took off from a trolley running along a track. Stabilized in flight by pre-set vacuum pneumatic and electrical controls the Kettering Aerial Torpedo would turn off its engines and release its wings, diving toward its target after a predetermined amount of time.

In the decade following the First World War not much more would be developed and investigated due to the armistice and a scarcity of funds. The next major developmental step would not come until the Second World War with the launch of the Fi-103, better known as the Vergeltungswaffe or V-1 in 1944. The V-1 was powered by a pulse-jet carrying a one ton warhead traveling around 560kph at 4,000ft with a range of 240km. This prompted America to develop their own long range UAV, the PB4Y-1 and BQ-7 which were converted Liberators and B-17's. These carried 25,000 pounds of explosives, flew via remote control using camera guidance systems, and were successful in knocking out V-1 launch sites – marking the first time UAV's were used against each other.

The Vietnam and Cold war in the 1960's, 70's and 80's saw a change in the role of UAV's. They moved from target drones and RPV (Remotely Piloted Vehicle) combat vehicles to reconnaissance vehicles. An example of this is the Lockheed D-21 from 1965. This was designed to be “stealth” and

had a top speed of Mach 4 and a ceiling of 80,000 feet.

UAV's continued their military involvement through the 90's. The 1990's realized the commercial viability of UAV's. The demand for technology items such as airbags in cars required high speed, low cost, small sensors with low power consumption that could also be used for unmanned flight. As people needed more information about the environment with greater accuracy UAV's such as the Pathfinder were developed, capable of flying for long periods of time at high altitudes collecting wind and weather information with very fine sensors and using high resolution digital cameras. One exciting development is Helios. Helios is intended to also be used as a broadband communications platform as a complement to satellite and terrestrial communication systems by flying continuously at 50,000 - 70,000 feet for months at a time.

As the century turned the technology required for autonomous flight rapidly became cheaper. Because of this the past two years have seen a rapid growth in autonomous projects. Today there are so many in development, with so much talk about them that a Goggle search for "UAV" returns 1,850,000 results. UAV's have recently been commissioned for disaster relief efforts, traffic monitoring, aerial mapping, and much more. Development groups include universities, aeronautical companies, military, and a few hobbyist groups worldwide.

The project name for this control system (Apeliotes) is the name of the God of the south east winds, from Greek mythology. Apeliotes is often depicted wearing gumboots with curly hair, a friendly expression, carrying fruit and draped in a light cloth concealing some flowers or grain since this wind caused a refreshing rain particularly beneficial to farmers¹. Apeliotes name was chosen because it seems to be relevant since New Zealand is located geographically in the South East of the world, is largely involved in farming, and also a weather and flight aspect is implied.

Apeliotes is a lightweight, low power magnetometer based unmanned aerial vehicle (UAV) flight control system. Apeliotes is a flight control system capable of flying a wide variety of unmanned model planes. To fly an aircraft must know its orientation. An attitude solution is vital for flight but can often be discounted by humans because they think that they know which way up is, but they don't. Not without looking that is. The inner ear canal will indicate which way is up for a short time. But if they close their eyes and turn around for some time, The person will soon loose track of the orientation of the world. That is until they open their eyes again. The horizon tells which way is up, while the floor and other objects tell which

¹Definition taken from Wikipedia online encyclopedia, written by Matthew Chave, 2005

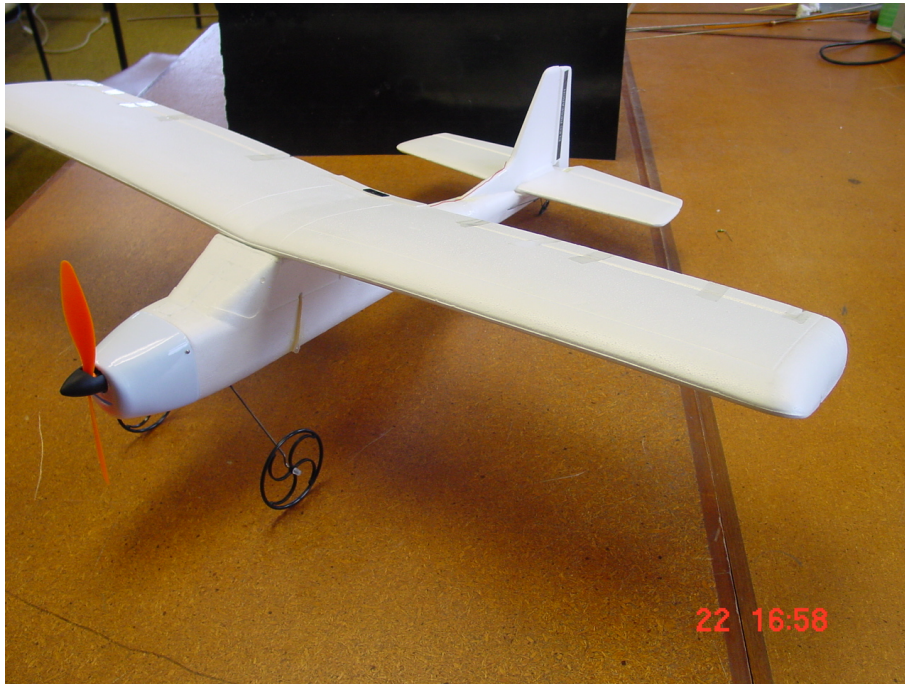


Figure 1.1: The GWS E-Starter airframe

direction the movement is in.

The attitude and position of a model aircraft comprise a state vector with six degrees of freedom. Apeliotes can incorporate magnetometers, accelerometers, gyros, pressure sensors and the Global positioning system (GPS) to calculate accurate position and attitude information.

A processor is used [2] to collect data from the sensors and calculate the current attitude and heading. This processor can then be used to control standard model R/C components such as servos and a speed controller to modify the state of the aircraft. This project is focused on the flight control system rather than the development of an airframe. For flight testing a GWS E-Starter was used, which is a standard low-cost electric model airframe (see Figure 1.1).

1.1 Overview

This report is formatted so that it takes the reader through the development process which Apeliotes went through. The initial design decisions, the circuit boards which were made, and then the required mathematics for the control system which could then be implemented. The reading is intended

to be pitched toward a student who is beginning research in this topic. This write-up attempts to maintain a functional level of understanding without diving too deep into problems such as the difficulties involved in implementing a fixed point math library etc. Apeliotes is interchangeably referred to throughout the report as: the autopilot, Apeliotes, UAV, and autonomous control.

Chapter 2

Design Considerations

The development choices for the electronics of the flight control system are outlined in this chapter. The block diagram in Figure 2.1 shows the systems overview.

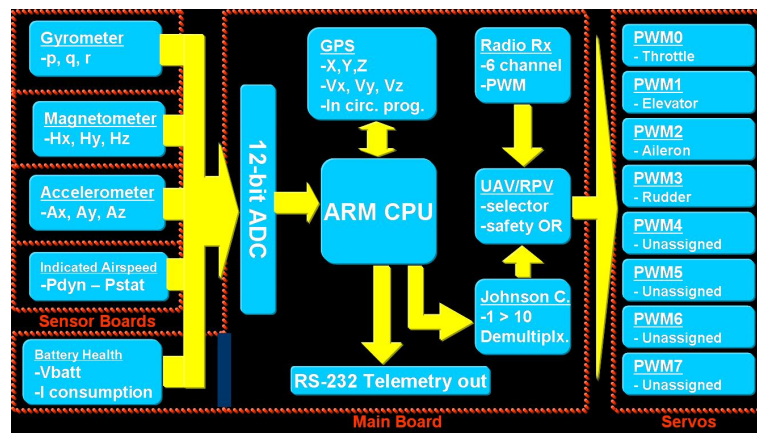


Figure 2.1: Hardware block diagram for UAV

2.1 Sensors

The selection of the sensors required was influenced by factors including price, availability, linearity, noise immunity, power consumption and weight. Figure 2.2 shows a photo of the sensors selected. Each of the sensors purpose is stated in this section.

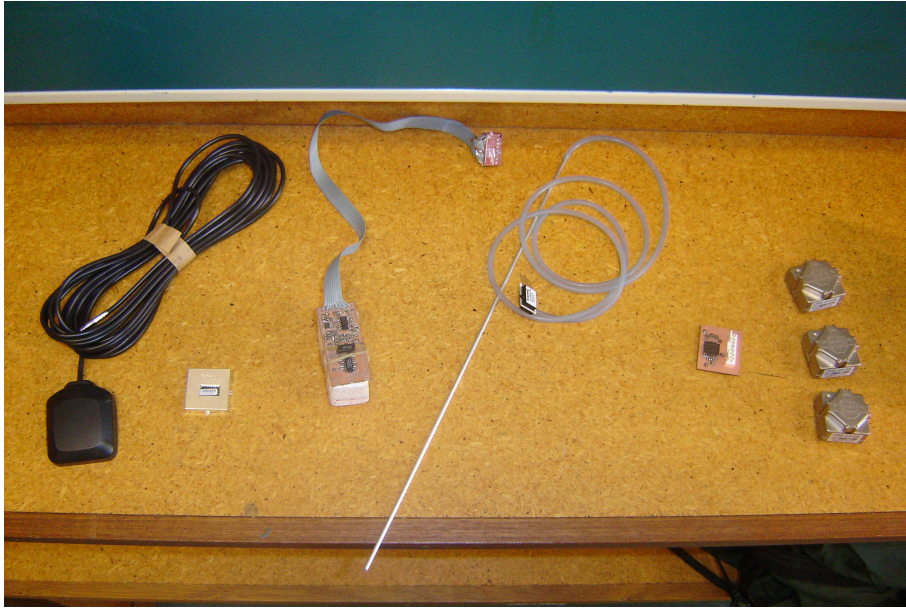


Figure 2.2: Sensors from left to right: GPS antenna, GPS module, magnetometers and pressure sensor, accelerometers, Gyros.

2.1.1 Attitude

The most important and elusive information needed to control an aircraft is the current attitude. The required attitude measurements are roll θ , pitch ϕ and heading ψ (also called yaw for simplicity although this is slightly incorrect). Inertial state inputs are typically integrated with respect to time giving the required attitude angles. This integration however is not reliable over long periods of time, typically larger than 30 seconds, due to the sensor drift and must be compensated and calibrated using other more reliable but slower reacting, or mathematically intensive sensors. Often the calibration for the inertial measurement unit (IMU) is achieved on a long time scale using other sensors such as the global positioning system (GPS), which has an update rate of 1Hz, sun sensing, star alignment, horizon sensing, accelerometers etc. This control system uses a three axis magnetometer and the worlds 12th order geo-magnetic model (which takes in date, altitude and geographic position). The model outputs a three axis magnetic field intensity, from which the direction vector of the local magnetic field can be established. Using this vector as a reference the magnetometers can measure the current magnetic field vector relative to the plane and calculate a quaternion rotation required to map the measured vector onto the reference vector (Chapter 4 describes this process). This magnetometer method will produce a result

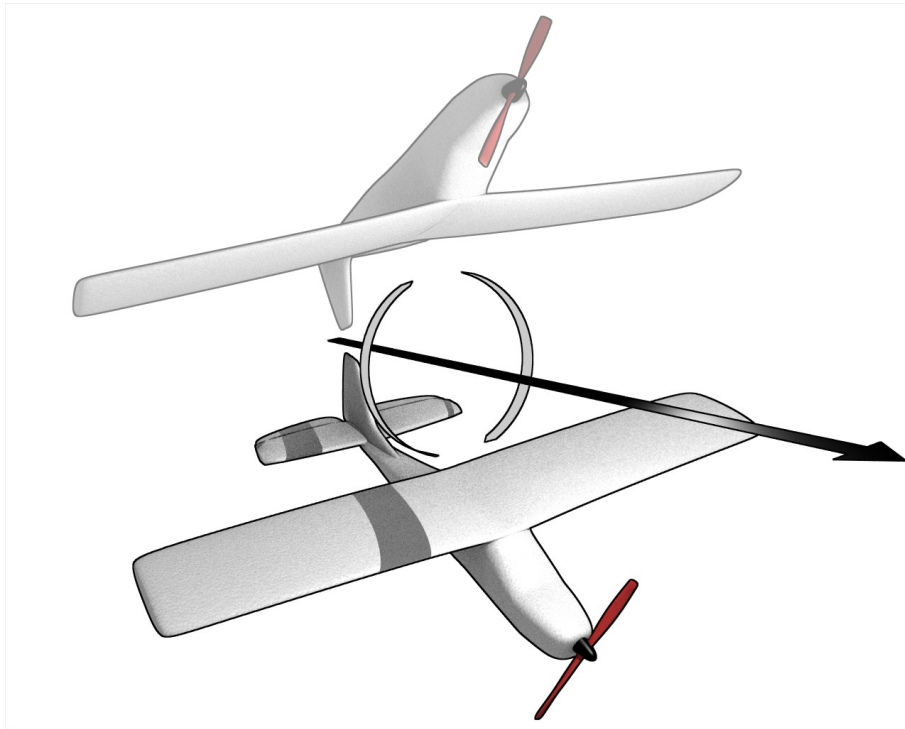


Figure 2.3: Rotations about the magnetic field vector produce the same readings [6]

for the attitude where the aircraft must be somewhere on the rotation about this calculated result graphically shown in figure 2.3. So we require the knowledge of one more rotation angle, for a complete solution. The airframe used has a large amount of dihedral and this project does not use ailerons so the roll can be assumed to be zero (see Section 5.6). So there will only be one position about the rotation which gives zero roll. Thus reducing the output requirements to just pitch and yaw. Which is discussed in Section 5.6.

2.1.2 Inertial State

“The innate force of matter [inertia], is a power of resisting, by which every body, as much as in it lies, endeavors to persevere in its present state, whether it be of rest, or of moving uniformly forward in a straight line.”[11]

As quoted Newton’s first law says that a body in motion will remain in motion unless acted upon by an external force. Inertial navigation is with

reference to coordinate frames. It is important therefore, to reference to an inertial (non-accelerating) frame. In aviation sensors are used to measure the rate of changes in position along and about a reference frames axis such as the body fixed axis of a plane. These measurements are then translated into an inertial reference frame where measurements are relative to the center of mass of the earth, the spin axis represents the z-axis, the x-axis can be measured with reference to star systems or where the sun crosses the equator during the equinox, then the y-axis is given according to the right hand triad [18]. For aviation navigation purposes a local level inertial reference frame is used where the axis are defined as NED or North East Down as positive directions and rotations according to the right hand rule [18].

Measurements are taken in the reference frame of the aircraft, called the Body frame since the sensors are carried on-board this approach is called the "strap down" method of inertial navigation. Measuring the inertial state of the aircraft's six degrees of freedom normally involves six inertial measurements including roll, pitch, yaw and translations along each of these directions, that is, accelerations and velocities along the three axes. Normally detected directly using rate gyros and accelerometers, it is necessary to use three of each requiring six more sensors to directly calculate the angular rates and the components of acceleration. Instead, sampling the three magnetometer axis at regular time intervals using a timed interrupt routine and calculating the rates of change is a more lightweight, cheaper, lower power option. This is also possibly a more reliable method, due to gyros and accelerometers being susceptible to drift.

2.1.3 Coordinated control

In large aircraft the coordination of a turn is indicated by an inclinometer. The inclinometer is a glass tube, filled with kerosene, with a free rolling steel ball (an example is shown in Figure 2.4). The tube is C-shaped; its center is the lowest point closest to the floor, each end being higher. During coordinated flight the ball will sit in the center of the tube, said to be centered [5]. The ball is used to indicate to the pilot if the required amount of rudder input is being used, during maneuvers such as rolls and turns.

While performing a roll maneuver if the ball deflects into the roll, then the rudder input is insufficient. Whereas if it deflects opposite the direction of the roll, the rudder input is excessive.

While performing a turn the ball is used to indicate if the rate of turn is correct for the current bank angle. If the ball deflects toward the direction of the turn, the aircraft is said to be in a slip, more inside (or 'bottom') rudder should be applied. If however the ball deflects toward the outside of the turn,



Figure 2.4: Aircraft inclinometer [14]

the aircraft is said to be in a skid, and more outside (or 'top') rudder should be applied.

The ball is a single axis accelerometer orientated along the y-axis of the aircraft (along the wings). Accelerometers can be implemented electronically using Micro-Electro-Mechanical Systems (MEMS) devices such as the Analog devices ADXL302. More accelerometers could be used to measure the loading along the three axis so that the aircraft is flown within the abilities of the airframe, gyros could also be used to measure rotation rates so that a complete closed-loop control system can be implemented for maneuvering the control surfaces (see Section 5.4.1).

2.1.4 Airspeed

Forward airspeed is a critical component in the flight of an aircraft. The control system must fly the aircraft within the envelope of the capabilities of the airframe. Which requires knowledge of the aircrafts stall speed and therefore knowing the aircrafts current airspeed is necessary. Several techniques were considered to sense air speed, which included:

- Heating two transistors to a constant temperature. One in the airflow the other not, and then calculating the difference in current required to maintain the temperature in each of the devices. This effect however requires complex calibrations and is potentially not very linear in the event of turbulent flows. This stands out as the cheapest solution.

- Propeller rotating in the airflow. The rate would be either sensed by current produced, or by counting the rotations using some kind of opto-couple or Hall Effect sensor. While not specifically part of the requirement of this project this technique will cause some inefficiency, is bulky and is the most mechanical of the solutions.
- Pitot tube. This uses a differential pressure sensor to take advantage of Bernoulli's principle to measure the difference in pressure between static and dynamic air pressure relative to the aircraft. This solution uses the most expensive components, however it extends to a large range of air velocities, requires very little drag, is not too difficult to calibrate and is the industry standard. For these reasons this technique was chosen.

2.1.5 Position Measurement

Position and average velocity measurements are determined using the Global Positioning System (GPS). The device used is a Trimble Lassen SQ GPS module. The velocity vector is the result of the aircraft's current heading (attitude) with environmental and airframe effects all relative to the earth. These effects could include, cross wind (see section 5.5.5 for cross wind compensation), or inaccuracies in the calibration for the attitude (see section 5.1.3 for calibrating the sensors) etc. The Trimble Lassen SQ GPS module uses the L1 frequency 1575.42 MHz, the C/A code, and continuous tracking of 8 satellites, with 32 correlations to achieve the parameters shown in table 2.1:

2.1.6 Battery health and current consumption

The plane converts energy from the stored chemical potential of the batteries or fuel into kinetic (velocity) and gravitational potential (altitude). This energy consumption and reserve must be monitored so that the control system can decide what to do given the current state of these energy reserves. The battery health and consumption is monitored using two of the ARM7TDMI-S CPU controller module's analog inputs. For battery health one input monitors a calibrated resistor pair which drops the voltage from the 9V of a healthy battery to 3V so that it is within a measurable range. Current consumption is monitored by passing the total supply current through a high power 0.003 Ohm resistor. The resulting voltage is then amplified using an AD8130 differential amplifier using suitably selected resistors so that the output voltage ranges from 0 to 3V for input to the ARM7TDMI-S CPU controller module's analog to digital converters.

| | |
|-----------------------|--|
| Power consumption | 110mW@3.3V |
| Update rates | TSIP@1Hz; NMEA@1HZ; TAIP@1HZ |
| Horizontal | < 6 meters (50%), < 9 meters (90%) |
| Altitude | < 11 meters (50%), < 18 meters (90%) |
| Velocity | 0.06 m/sec |
| PPS | 95 nanoseconds |
| Reacquisition | < 2 sec. (90%) |
| Hot start | < 14 sec (50%), < 18sec (90%) |
| Warm start | < 38 sec (50%), < 45sec (90%) |
| Cold start | < 90 sec (50%), < 170 sec (90%) |
| Dynamics | Acceleration : 4g (39.2m/sec ²) |
| Motional jerk | 20 m/sec ³ |
| Operational Limits | Altitude < 18000m or velocity < 515 m/s (COCOM limit) Either limit may be exceeded but not both |
| Connectors | Antenna -RF Low profile coaxial connector 1 serial port (transmit/receive) |
| Operating Temperature | -40C ≤ T ≤ +85C |
| Vibration | 0.008 g ² /Hz @ 5Hz to 20Hz 0.05 g ² /Hz @ 20Hz to 100Hz ± 3 dB/octave @100 Hz to 900 Hz |
| Operating Humidity | 5% to 95% R.H. non-condensing @ +60C |
| Weight | Approximately 5.7 grams (0.2 ounce) |

Table 2.1: Trimble Lassen SQ parameters (from [8])

2.2 Support Hardware

This section describes the separate integrated circuit's (IC's) used to interface to the sensors, servos, radio receiver, etc to the processor, including the selection of this processor.

2.2.1 Analog input

The sensors supported by the control system require 13 analog inputs, the processor core contains 4 analog to digital converters (ADC), of which two are unavailable due to their other functionality (see [15] for the pin-out information of the processor). The large number of analog inputs could be multiplexed into the available pins but this would require routing past the noisy digital signals on the main board and would still require at least one

extra integrated circuit (IC). To resolve this problem a dedicated ADC IC was selected. The ADC chosen was the MAXIM, MAX1231. This IC is capable of sampling 16 inputs at a total of 300ksps. The internal reference temperature input would mean that an easily accessible analog input would be readily available when it was time for programming, and also provides a means for main board temperature measurement. The chosen ADC has an accuracy of 12-bits which gives a resolution of approximately $3V / 4095$ which is 0.733mV. For the attitude reference from the magnetometers this would mean an ADC resolution of approximately 0.9 degrees which is adequate. The digital interface provided uses the SPI (Serial Peripheral Interface) protocol which will use six pins to talk to the processor. The SPI interface is desirable because it is implemented in hardware on the chosen processor, so therefore transparent to the users processor tasks. For further functionality of the MAX1231 see [9].

2.2.2 Mode selection UAV/RPV

The autopilot must have a way of being disabled so that a human pilot can take over the control of the aircraft. This is useful for testing small parts of the control system incrementally (see chapter 7 for testing). The UAV/RPV (Unmanned Air Vehicle/Remotely Piloted Vehicle) selector is attached to the fourth channel of the RC transmitter. The selection works using a data latch setup so that as the rising edge of the signal from the receiver is detected this starts a timer (MC4013B for the timer and D latch). This timer counts for a time which can be modified by rotating the variable resistor on the main board. Typically the length of this timer would be 1.5ms which represents the transmitters stick in the center position. When the time is reached the pulse level from the receiver is latched. If the signal is still high then the Q value output from the data latch will be high and so the octal buffer/line driver (74LS541DW) which has its chip select attached to this line will be on, while the octal buffer/line driver which has its enable line attached to the Q bar output will be disabled. The state of the system can immediately be seen by the red indication LED (Light Emitting Diode) located next to the power switch. The circuit is shown in Figure 2.5

2.2.3 (De)Multiplexing the controller to servo output

The servos each require a pulse of varying width about 1.5ms at least every 30ms. The control system currently has 8 servo outputs which it talks to using a Johnson counter (MC14017BD). The Johnson counter uses two inputs CLK and RESET and is capable of driving 10 outputs, it can also be daisy

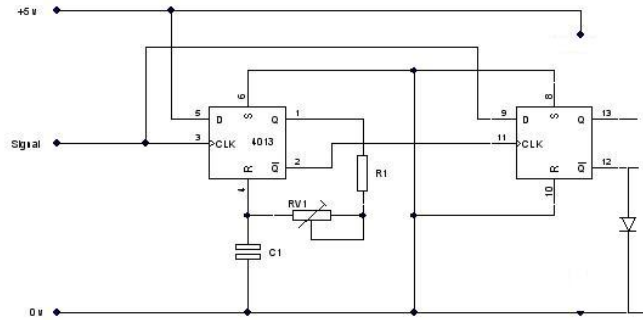


Figure 2.5: UAV/RPV switch

chained so that this number can be what ever is required. For this system 8 servo outputs should be more than enough, 8 was chosen because there were 8 line driver input and outputs and also the 8 outputs could be, for example, Rudder, aileron, elevator, throttle, gear, flaps this would use all the outputs depending in the layout selected and the level of control required. The control system uses a low overhead interrupt routine so that the processor is not always busy counting in a delay loop. The interrupt routine is triggered by one of the processors timers which is reset then loaded with four values to count to. Upon reaching each value the interrupt routine is triggered which outputs a short pulse to the Johnson counter. Once the internal timer matches the fourth value the next four servos values are loaded into the timer match registers and the timer is reset. When the timer matches the fourth value this time around the Johnson counter is reset along with the timer and the new first four servo values are loaded into the timers match registers, repeating the process approximately every 16ms. The Johnson counter takes in this serial data stream and changes the state of two neighboring output pins simultaneously on each rising edge of the CLK signal. Once a reset is issued the Johnson counter drives all of its outputs to low except for output zero which is driven high. Now when the reset line is set back low and a CLK rising edge is detected the zeroth output will change state to low and the first output will become high. So the controller should send a pulse which returns to low so that the controller is ready to issue the triggering signal as soon as the time value is correct. The timing diagram for this process is shown in Figure 2.6

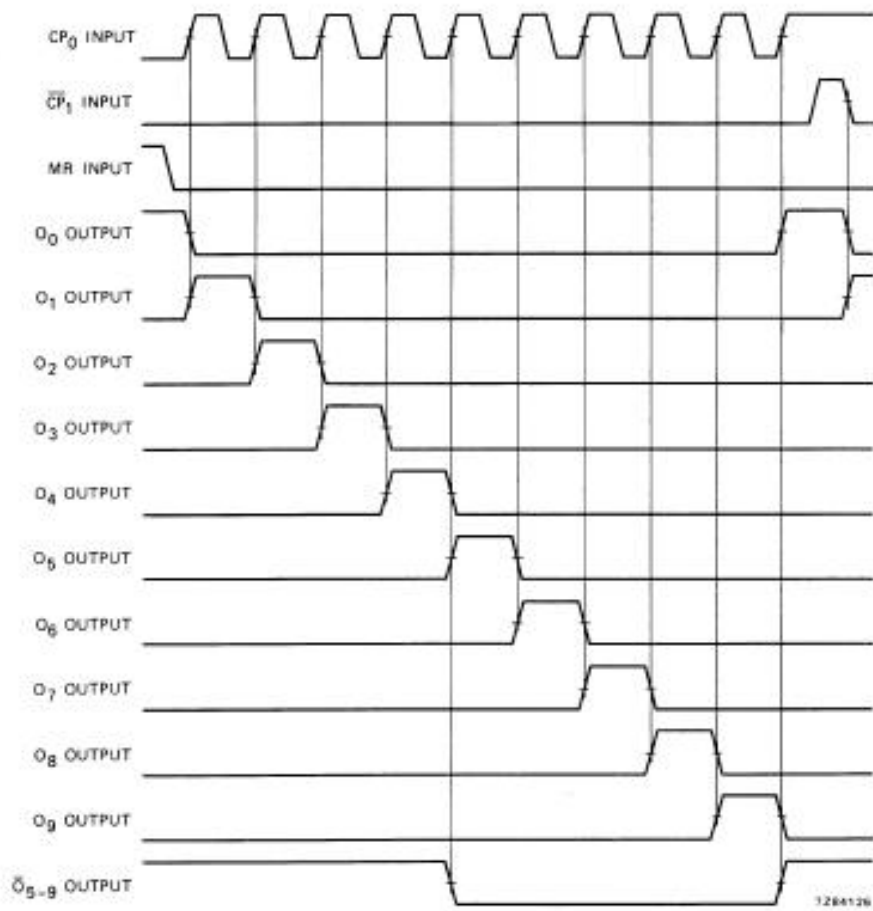


Figure 2.6: Timing Diagram for the Johnson counter from [16]

2.3 The processor

The system designed uses one processor to compute everything required for autonomous flight. This includes; attitude and navigation solutions, software filtering, aircraft control and telemetry so a powerful processor is required. The processor needs also to be small, light weight and energy efficient so that no bulky cooling solutions are required and battery longevity is reasonable.

To fulfill these requirements an ARM7TDMI-S high end micro-controller module [2] was selected. This processor has the following specifications:

- Phillips LPC2129 ARM7-TDMI micro-controller.
- Better than 1mW / MIPS (milliwatts per million instructions per second).
- ARM7 core from Advanced RISC Machines.
- 32-bit RISC (Reduced Instruction Set Computer).
- Board size of 51mm x 29mm.
- Low cost.
- 3.6 to 5.5V supply voltage, with on-board 1.8V and 3.3V supplies, the 3.3V supply being capable of supplying 300mA of current.
- 14.7456 MHz oscillator clock with a 1, 2, 3, or 4 times multiplier which is dynamically selectable for power on demand (such as could be required upon reaching a waypoint).
- 60 MHz maximum clock rate, with 1 instruction per cycle.
- Socket-able via two dual row 40 pin 1.27mm headers

Chapter 3

PCB Design and Layout

The design constraints for the circuit board where to minimize crosstalk where necessary, minimize size, minimize the time spent to get something to work and layout the board so that it is balanced and the components can be easily plugged in while still making the necessary components accessible to the operator.

3.1 Main Board

A photo of the fully assembled main PCB is shown in Figure 3.1 with the board layout detailed in Figure 3.2. The board is laid out so that the analog data is as far away as possible from the digital data with a ground plane running underneath. The servo outputs are grouped together on the side of the board, with the ARM processor module in the center. The power input, switches and sensing are at the end opposite the analog to digital converter. The 8 header switches are accessible for reversing the direction of the individual servo outputs. The board is oblong shaped so that it will easily fit into most model sized aircrafts fuselages.

3.2 Sensors

3.2.1 Triaxial magnetometer

The magnetometer board has the sensing, filtering and amplification stages for the magnetic field implemented. The magnetic field sensors used are Honeywell magneto-resistive devices, internally configured as a Wheatstone bridge. These small and low cost sensors are capable of sensing magnetic fields as low as $30\mu\text{gauss}$ with a field range up to $\pm 6\text{gauss}$, where the earths

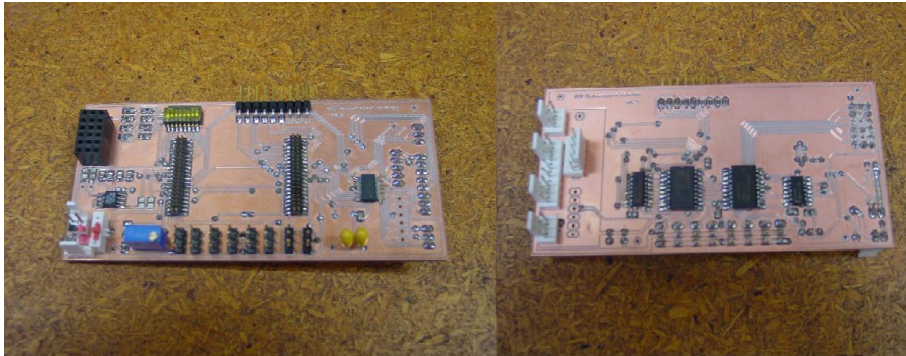


Figure 3.1: Fully assembled main board, the 40 pin connectors are for the ARM module

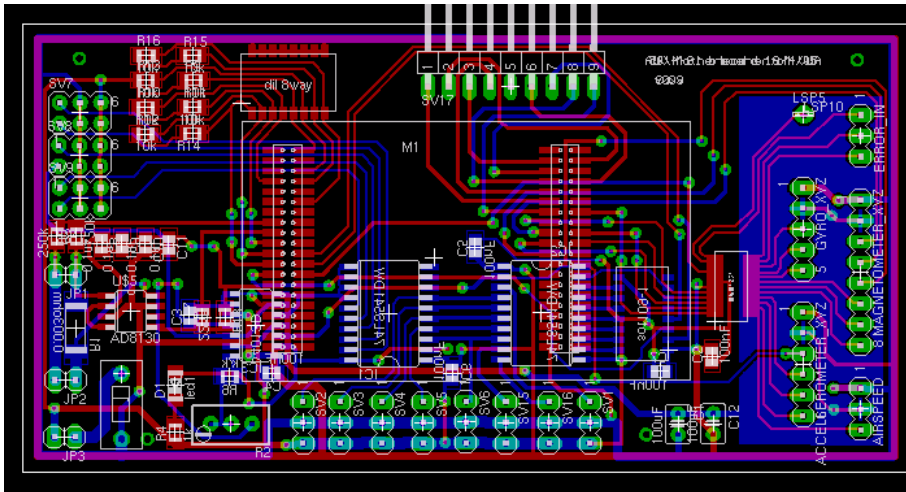


Figure 3.2: Eagle Board design picture

field is approximately 0.5gauss . The sensors used in this circuit are the HMC1022 2-axes sensor, and the HMC1021Z single axes sensor.

This sensor board is connected to the main board via an 8 pin cable. The cable carries the supply voltages for the on-board circuitry, the reset line for the magnetometers and the amplified analog signals for input to the main board. This board is designed to be very small so that it may be placed in the tail of the aircraft away from the engine noise, without affecting the weight distribution of a small aircraft too much.

Figure 3.3 shows the design of the board at what should be the actual size, and Figure 3.4 shows a photo of the assembled board. The magnetometer sensors consume approximately 50mW each, for a combined 150mW across the 3-axes.

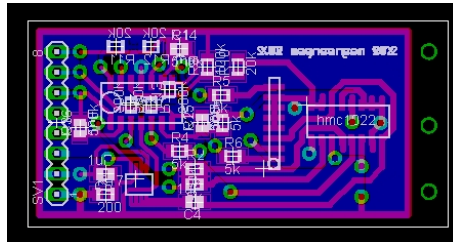


Figure 3.3: 3 axis magnetic field board design layout, measuring 5cm by 2cm

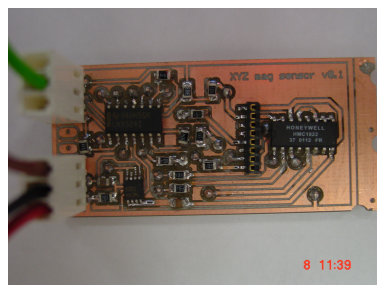


Figure 3.4: 3 axis magnetic field sensor board

Chapter 4

Magnetometer Attitude Determination

Determining attitude information from a magnetic field vector can be achieved by two main methods. Some micro and nano satellites use magnetometers to calculate the rate of change of the magnetic field vector about the three axes. The rate of change is then integrated over time through an extended Kalman filter (for more information on Kalman filters see [3]) to give an estimation of the crafts current attitude. This method does not require any prior mapping or modeling of the local magnetic field vector since only rates of change are measured. The second method, the method which is used here for Apeliotes, takes advantage of the earths geomagnetic field being well mapped and modeled. This second method uses a local earth referenced calculated magnetic field to compare with the body referenced measured field to determine the current attitude of the aircraft. This chapter describes how this second method is achieved.

4.1 Local reference magnetic field calculation

Accurate models of the earths magnetic field have become extremely accurate due to the extensive work carried out by The International Association of Geomagnetism and Aeronomy (IAGA), the United States National Geophysical Data Center (NGDC), and the British Geophysical Survey (BGS) [10]. Their interests for modeling and collecting data on the magnetic field include study of the earths deep interior, crust, ionosphere, and magnetosphere.

The model developed to date uses a thirteen degree and order spherical harmonic approximation as shown by Gauss in 1839, with coordinate transformations as outlined by the World Geodetic System 1984 (WGS84) [17].

The parameters for the WGS84 are

a = 6378.137 km and
b = 6356.752 km

To adjust for the time varying components the mathematical models of the Earth's main field track its annual rate of change (secular variation). In source-free regions at the Earth's surface and above, the main field, with sources internal to the Earth, is the negative gradient of a scalar potential V which can be represented by a truncated series expansion:

$$V(\gamma, \theta, \lambda, t) = R \sum_{n=1}^N \left(\frac{R}{r}\right)^{n+1} \sum_{m=0}^n (g_n^m(t) \cos m\lambda + h_n^m(t) \sin m\lambda) P_n^m(\theta) \quad [10]$$

where r , θ , λ are geocentric coordinates (r is the distance from the center of the Earth, θ is the co-latitude, i.e. 90 - latitude, and λ is the longitude), R is a reference radius (6371.2 km). $g_n^m(t)$ and $h_n^m(t)$ are the coefficients at time t and $P_n^m(\theta)$ are the Schmidt semi-normalized associated Legendre functions of degree n and order m . The maximum spherical harmonic degree of the expansion is N . The coefficients are functions of time which are assumed to have linear change over five-year intervals, since the magnetic field is not yet fully understood these coefficients are updated every five years. For the upcoming five-year epoch, the rate of change is given by predictive secular variation coefficients (for further reading on the modeling process see [4, 13]).

The International Geomagnetic Reference Field's (IGRF) magnetic field values currently have a precision of 0.1nano-Tesla (nT). This is approximately one hundred thousandth the size of the earths magnetic field which is about 10000nT. The IGRF model coefficients and source code (available in C and FORTRAN) are available freely for download on the internet from the IAGA's website.

The model took as its inputs:

- Geocentric or Corrected GeoMagnetic Latitude and Longitude
- Altitude above the earths surface at 6371.2 km with a 40,000 km ceiling
- Year for Definitive/International Geomagnetic Reference Field (DGRF/IGRF)

Giving the following outputs:

- Total magnetic field intensity in nT

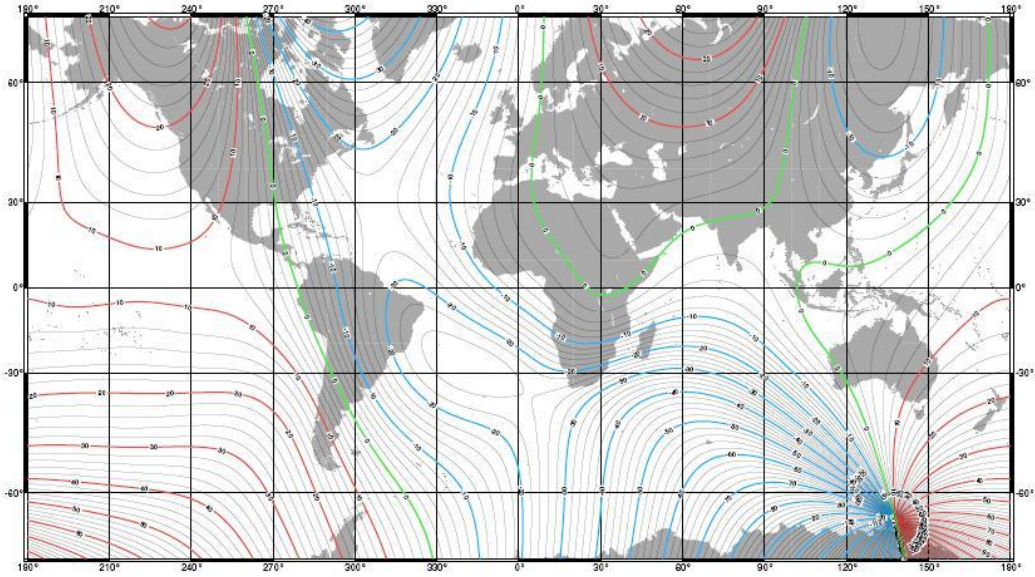


Figure 4.1: World map of the magnetic declination as of 2005, in degrees with contour interval of 2 degrees [12]

- Horizontal magnetic field intensity in nT
- North Magnetic field intensity in nT
- East Magnetic field intensity in nT
- Down (vertical) Magnetic field intensity in nT
- Magnetic field inclination in degrees
- Magnetic field declination in degrees (see Figure 4.1)

4.2 Body referenced magnetic field given desired attitude

Now that the co-ordinates of the magnetic field in the earth referenced frame are known \vec{B}_e , it must be combined with the current desired attitude. This produces a vector which should be equal to that measured by the magnetic field sensors when the aircraft is flying with the desired attitude. The transformation between the earth referenced field and the body referenced field is done using quaternions (see Appendix A). Quaternions are used because

they are a computationally efficient and logical way of handling rotations. The Quaternion operates by producing a vector which when rotated around by a determined amount will map a second vector onto a third vector. This single rotation removes the ambiguity which is present in Euler angles due to them being non-commutative (see [7]).

The Euler attitudes θ , ϕ and ψ are combined into quaternions as follows:

$$\begin{aligned} q_\theta &= \left(\cos\frac{\theta}{2}, \sin\frac{\theta}{2}, 0, 0\right) \\ q_\phi &= \left(\cos\frac{\phi}{2}, 0, \sin\frac{\phi}{2}, 0\right) \\ q_\psi &= \left(\cos\frac{\psi}{2}, 0, 0, \sin\frac{\psi}{2}\right) \end{aligned}$$

The quaternions are multiplied together to produce total rotation,

$$q_T = q_\theta q_\phi q_\psi$$

See Appendix A.1 for details on quaternion multiplication. The final rotation quaternion is then,

$$q_T = \begin{pmatrix} \cos\frac{\theta}{2}\cos\frac{\phi}{2}\cos\frac{\psi}{2} & -\sin\frac{\theta}{2}\sin\frac{\phi}{2}\sin\frac{\psi}{2} \\ i * \sin\frac{\theta}{2}\sin\frac{\phi}{2}\cos\frac{\psi}{2} & + i * \cos\frac{\theta}{2}\sin\frac{\phi}{2}\cos\frac{\psi}{2} \\ j * \cos\frac{\theta}{2}\sin\frac{\phi}{2}\cos\frac{\psi}{2} & - j * \sin\frac{\theta}{2}\cos\frac{\phi}{2}\sin\frac{\psi}{2} \\ k * \cos\frac{\theta}{2}\cos\frac{\phi}{2}\sin\frac{\psi}{2} & + k * \sin\frac{\theta}{2}\sin\frac{\phi}{2}\cos\frac{\psi}{2} \end{pmatrix}$$

Applying this rotation quaternion to the reference field vector \vec{B}_e rotates the zero attitude vector to the desired attitudes body referenced vector,

$$\underline{B}_{desired} = q_T \underline{B}_{zero\ attitude} q_T^*$$

Where q_T is a unit vector $q_T * (w, i, j, k) = q_T(w, -i, -j, -k)$ so that the imaginary parts are just reversed in sign. Then we get the final result (see Appendix B.1 for combined example code)

```
x_field =
Ta*Ta>trueN_field.x + 2*Tc*Ta>trueN_field.z - 2*Td*Ta>trueN_field.y +
Tb*Tb>trueN_field.x + 2*Tc*Tb>trueN_field.y + 2*Td*Tb>trueN_field.z -
T3*T3>trueN_field.x - Tc*Tc>trueN_field.x;
```

```
y_field =
2*Tb*Tc>trueN_field.x + Tc*Tc>trueN_field.y + 2*Td*Tc>trueN_field.z +
2*Ta*Td>trueN_field.x - Td*Td>trueN_field.y + Ta*Ta>trueN_field.y -
```

```

2*Tb*Ta>trueN_field.z - Tb*Tb>trueN_field.y;

z_field =
2*Tb*Td>trueN_field.x + 2*Tc*Td>trueN_field.y + Td*Td>trueN_field.z -
2*Ta*Tc>trueN_field.x - Tc*Tc>trueN_field.z + 2*Ta*Tb>trueN_field.y -
Tb*Tb>trueN_field.z + Ta*Ta>trueN_field.z;

```

where Ta, Tb, Tc and Td denote the four terms of the defined rotation quaternion. trueN_field.axis denotes the field measured along the denoted axis when the aircraft has zero attitude (i.e zero roll, pitch and heading). Finally axis_field denotes the body referenced magnetic fields for a given attitude as defined by θ , ϕ and ψ earlier.

4.3 Calculating rotation to achieve desired attitude

Now that a reference vector has been established, which is what should be measured if the plane has the desired attitude, the current magnetic field must be measured. This is done using the 3-axis magnetometer described in 3.2.1.

The vector is measured with reference to the aircraft (Body frame) so any rotations about this measured vector produce exactly the same measurement, Figure 2.3 helps visualize this. Therefore we can only calculate two rotations without using any other sensors such as more magnetometers or horizon sensors. However if we can assume that there is zero roll (valid for the current airframe when not turning, see section 5.6) so that one of the three rotations is removed, then the heading and pitch rotations can be resolved. There are two important exceptions here, the first is that at the poles (magnetic poles) the heading is undefined. The second case is that at the magnetic equator when flying along this equator the pitch is undefined due to a zero intensity in the X-Z plane, the heading also measures the same either in the east or west direction (one way is flying upside down). These are the only obvious failures. All other locations and attitudes do not have these problems because the known roll measurement means that only one solution is available.

So if the body referenced observed magnetic field is measured to be M_x , M_y , M_z then the rotation Q_w , Q_i , Q_j and Q_k required to map to the desired field D_x , D_y and D_z is

$$Q = Q_M(0, M_x, M_y, M_z) \times Q_D(0, D_x, D_y, D_z)$$

The final result for the Quaternion rotation which would map the current aircrafts attitude to the desired aircrafts attitude turns out to be.


```
q0 = -trueN_field.x*observed_field.x - trueN_field.y*observed_field.y  
- trueN_field.z*observed_field.z;  
q1 = trueN_field.y*observed_field.z - trueN_field.z*observed_field.y;  
q2 = -trueN_field.x*observed_field.z + trueN_field.z*observed_field.x;  
q3 = trueN_field.x*observed_field.y - trueN_field.y*observed_field.x;
```

Excerpts from the source code can be found in Appendix B.3 with multiplication from Appendix A.1.

Chapter 5

Flight Control System

The flight control system uses the sensor information as feedback, performing attitude estimation to set the control surfaces of the aircraft as output to change the orientation of the aircraft to the desired attitude (Figure 5.1). This chapter describes how this process is performed.

5.1 Sensor measurement

5.1.1 Conditioning

Conditioning of the signals which come from the sensors is necessary since they are often noisy and small in amplitude. The magnetometers are placed as far away as possible from the engine and main board. Ideally this long range link should be digital so that it is more immune to noise however this is not yet implemented. The analog signals can be filtered using a simple second order low pass Butterworth filter such as that in 5.2.

With the component values of :

- $R1 = 50 \Omega$
- $R2 = 50 \Omega$
- $L1 = 0.375075 H$
- $C1 = 0.00015003 F$

To produce a 50Ω input impedance, and a frequency profile as shown in 5.3 which has a reasonable cutoff for frequencies above 20 Hz. Twenty Hertz was chosen because some model aircraft are capable of doing a complete revolution in fractions of a second and so a reasonable bandwidth is necessary,

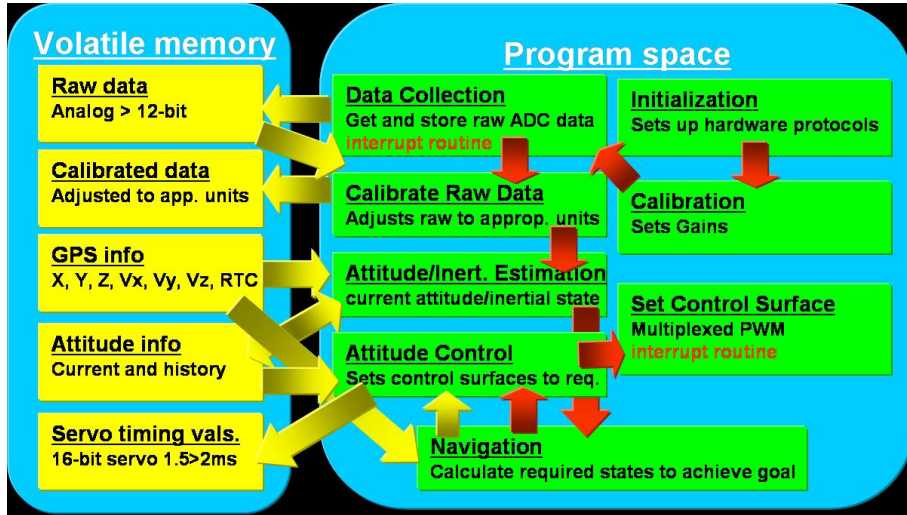


Figure 5.1: Implementation of the control system

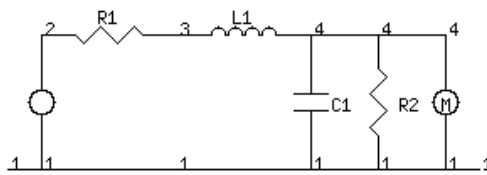


Figure 5.2: Second order low pass butterworth filter

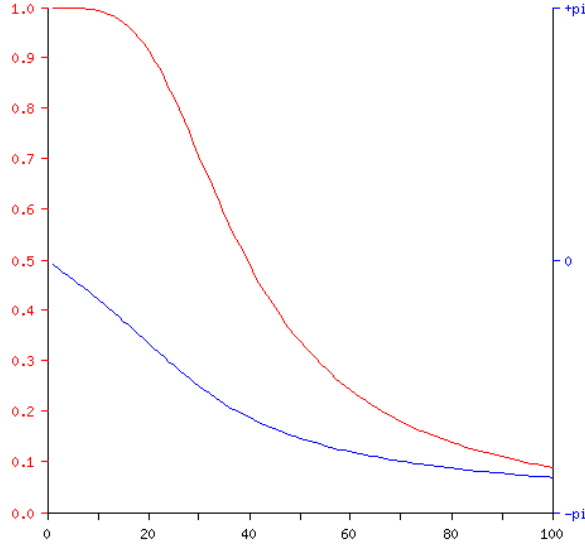


Figure 5.3: Spice simulated filter, red represents amplitude, blue phase, with frequency horizontal.

but we are not really interested in oscillations above 20 Hz as the aircraft which would be chosen will have a reasonable amount of inherent stability.

The signals are then amplified using a non-inverting amplifier (5.4). The Non-Inverting Amplifier multiplies the input voltage, V_{in} by the desired positive gain, and subtracts a voltage proportional to the applied reference voltage:

$$V_{out} = V_{in}x(1 + R_f/R_g) - V_{ref}x(R_f/R_g)$$

Where the feedback capacitor C_f rolls off the gain at frequencies above $\frac{1}{2\pi} \times R_f C_f$, to attenuate high-frequency noise.

The following values were chosen for the components of the magnetometer amplifiers:

- $A1 = \text{LMV324}$
- $C_f = 0.002400 \text{ uF}$
- $R_f = 196000 \ \Omega$
- $R_g = 2000 \ \Omega$

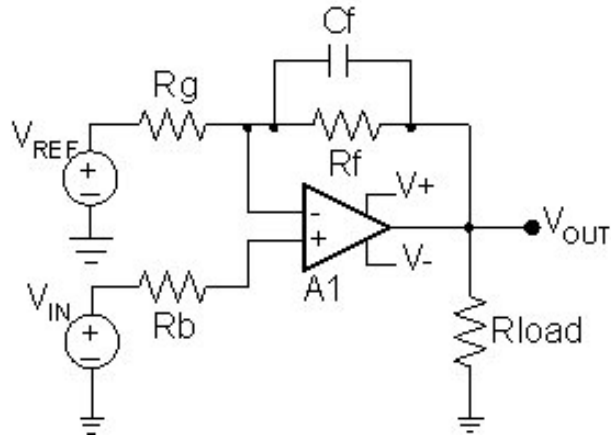


Figure 5.4: Non-Inverting amplifier schematic

5.1.2 Sampling

The analog signal is sampled by an analog to digital converter (described in Section 2.2.1). The data is sampled inside the ADC and averaged over 32 samples. Currently this sampling process is called from within the code whenever readings are needed, but in the future should be done at a pre-determined time interval such as every 25ms using an interrupt routine. Then the signal can be mathematically operated on, such as integrated, because the time intervals of the samples are known. Sampling at 40 Hz gives a signal frequency detection of up to the pre-determined 20 Hz.

5.1.3 Calibration

The calibration process is currently required because many of the components are not perfect. For example the magnetometers each respond to the magnetic field with some varying degree of accuracy and offset, the amplifiers do not all have the same gain and the signals are attenuated slightly differently as they propagate through to the ADC. So the signals must each have an offset value and a gain associated with them. These are calculated using the following process:

- Set the flag in the UAV.cpp code for calibration output. This outputs serial data down the secondary RS232 port on the side of the main board. The format is: Xfield XfieldMIN XfieldMAX Yfield YfieldMIN YfieldMAX Zfield ZfieldMIN ZfieldMAX
- The operator must then orientate the aircraft while monitoring the output values to try and maximize and minimize the appropriate results.

- Now the offsets and gains can be calculated using the following formulas

$$Offset = \frac{max - min}{2} + min$$

$$Gain = \frac{Greatest(max - min)}{max - min}$$

- Now the operator must adjust the appropriate variables found in magnetometer.h for the new values.

The calibration is a once off operation which takes around 20 minutes. The values must be recalculated when relevant components of the board are modified, or for the magnetometers, if the airframe is modified in such a way that the magnetic field would be effected. The values should be stored for future reference.

5.2 Attitude detection

Using the magnetic field and quaternion rotation method described in section 4 the attitude of the plane can be deduced. The practical implementation is fairly simple. The magnetometers are mounted on a rigid mount near the tail of the airframe, so that all attitudes calculated are with reference to this mounting location. Using the magnetometer attitude method, the sensor does not need to be mounted close to any of the rotation axis of the plane since there is no coupling from the movement as there is for accelerometers and gyros. So the mounting location can be anywhere most convenient, preferably away from noise sources. Since the values which come from the sensors go through a significant amount of mathematical manipulation their values are modified so that they are close to unary. The attitude values are then stored in specific memory locations accessible by other parts of the code.

5.3 Output

The control system electronically outputs to the outside world using three types of communications; 2-wire serial data for the control surfaces, RS-232 for the GPS and telemetry/debugging, and SPI

5.3.1 Servo output

The servos each require a pulse of varying width about 1.5ms at least every 30ms. The control system currently has 8 servo outputs which it talks to using the Johnson counter. The Johnson counter uses two inputs CLK and RESET. To output the 8 required signals the control system uses a low overhead interrupt routine so that the processor is not always busy counting in a delay loop. The interrupt routine is triggered by one of the processors timers which is reset then loaded with four values to count to. Upon reaching each value the interrupt routine is triggered which outputs a short pulse to the Johnson counter. Once the internal timer matches the fourth value the next four servos values are loaded into the timer match registers and the timer is reset. When the timer matches the fourth value this time around the Johnson counter is reset along with the timer and the new first four servo values are loaded into the timers match registers, repeating the process approximately every 16ms.

5.3.2 Telemetry/Debugging output

The control system is capable of outputting and inputting data using a fully functional serial RS232 port. The 9-pin plug on the side of the motherboard is used to plug into (also the GPS port on top of the processor can be used). This port is useful for outputting debugging information while developing the on-board code. While ground testing the control system the port can be used to output telemetry information. While in flight the port can be used to plug a data logger or a modem to capture the telemetry for display on the ground.

5.3.3 SPI communication for ADC and miscellaneous on-board packages

The main board uses an SPI protocol to communicate with the ADC and is available for any additional on board packages use via a five pin header on the main board. This is a high speed serial communications protocol capable of sending and receiving full-duplex data at a 40MHz clock rate.

5.4 Simple first approach

For this control system a first order proportional control is used. Apeliotes currently uses the first, P part, of a PID (proportional, integral, and deriva-

tive) algorithm. A PID algorithm takes a reference value measures an input and attempts to drive an output to the desired reference value. Meanwhile the input is continually manipulated by external influences, and the output of the PID controller. The P is implemented only at the moment to obtain the systems response to determine what needs to be improved by adding the I and D components.

5.4.1 PID control

Proportional

The components of a PID algorithm are all driven by the difference between the process value and the reference value. This difference is the current error in the state of the aircraft. For a particular time step this error can be denoted e_n . For the same time step, the process value is y_n and the reference point r_n .

$$e_n = r_n - y_n$$

The output value requested is called u_n . Proportional control simply calculates u_n based on the magnitude of the error e_n by multiplying it by a constant, K_P .

$$u_p = K_P \times e_n$$

Only using this for the control algorithm will produce satisfactory results for an initial attempt. Proportion only control will work provided that when $e_n = 0$ then $u_n = 0$. So the aircraft needs to be trimmed correctly when only using this control. The trim is adjusted using a servo control function which is preset for the desired trim signal for each servo.

Integral

Where the aircraft is not perfectly trimmed and in most cases it wont be, since the amount of control surface deflection needed to drive the error to zero can vary with speed, a proportional only controller may stabilize out quickly, but probably to the wrong value. So to drive the error to zero the Integral component of the PID algorithm will be required. This is the area error under the process curve. If each time step of e_n is known, then by multiplying this error by the time step dt an area is calculated which approximates the error under the curve for this time step. If the areas are summed over time the result is a reasonable approximation of the area under the curve.

$$u_i = K_I \times \sum_{n=1}^n e_n \times dt$$

So the longer time passes that the target value is not achieved, the larger that the sum of the difference becomes over time. If this sum is used to push the output value then the more time that passes that the target is not achieved, the more the system forces the output. So the integral can compensate for the trim error in the proportional component and the system will stabilize out with the desired value.

derivative

The derivative function gives the rate of change of the measured input. This rate of change gives how fast the system is converging (or not converging) on the target value.

$$u_d = K_D \times \frac{de_n}{dt}$$

So here the amount of output is proportional to the rate of change in the input.

combining the three

Now a more stable controller can be built capable of achieving the target value at an optimum rate for an accepted level of oscillation about this target.

A proportional only controller is stable but can stabilize to the wrong value. An integral only controller will quickly hit the target value, but will overshoot, then overcompensate, oscillating about the target value. Whereas a derivative only controller would drive the output further in the direction of the changing error without knowing the target set point. The I and D components are unstable.

The trick then is to combine these components together by summing them. The actual output is equal to what the P component says the output should be plus what the I component says the output should be plus what the D component says the output should be.

$$u_n = u_p + u_i + u_d$$

While the math involved in a PID controller is quite simple to implement. The trick for creating a well behaved control system is tuning the relative weights K_P , K_I and K_D of each of their respective P, I and D components.

5.4.2 Attitude Control

Roll, Pitch and Heading constitute the three degrees of rotation and the way in which they can be immediately modified is by using Aileron, Elevator and Rudder respectively. Since the quaternion rotation required to map the measured attitude to the commanded attitude is known then the control system has every thing it needs to know. Since it has already calculated:

$$q = \cos\left(\frac{\Omega}{2}\right) + i(x * \sin\left(\frac{\Omega}{2}\right)) + j(y * \sin\left(\frac{\Omega}{2}\right)) + k(z * \sin\left(\frac{\Omega}{2}\right))$$

Where x , y and z represent a unit vector, about which we are rotating. So since this is the axis of rotation then this is the error vector e_n about which the plane should turn. If the vector is all in the z axis then the plane needs to do a yaw rotation using the rudder. If the vector is completely in the y axis then the plane needs to perform a rotation using its elevators. These rotations are combined to cover all the combinations of attitudes. The total amount of rotation required is given by the real term and the lengths of the respective axis. This measurement is used as an error magnitude e_n , about the respective axis components and fed into the servo controller, a function called `calc_control()`. Which takes into account the airframes responsiveness about each axis by applying a preset gain value K as per section 5.4.1. This gain value is currently calculated by the operator for each airframe by a trail and error process. The GWS E-Starter's values can be seen in B.4.

5.4.3 Simple turn

A turn is currently commanded by rotating the reference field vector as per section 4.2. This causes an error between the measured vector and this reference vector and so a rotation is calculated. This rotation is then used as an error signal e_n which feeds through as described above in section 5.4.1.

5.5 Navigation

In order to have the full functionality of an autonomous vehicle the aircraft must be capable of navigation. This section describes how navigation is intended to be done. However, although most of the coding has been done (for example see Section B.5). The navigation algorithms discussed here are not on the current version of the control system.

5.5.1 Measuring the current location

To measure the current location a standard GPS OEM module is used as per section 2.1.5. This module is capable of measuring the aircrafts absolute position to within an error of 10m. So this should be taken in to consideration when setting criterion for the waypoints.

5.5.2 Waypoints

The waypoints are to be hand selected by the operator. These could be chosen from topographical mapping software and typed into a table which is uploaded onto the control system. The plane must be able to achieve the waypoints to within some accuracy so careful selection and planning must be used.

5.5.3 Achieving way points

A waypoint is to be determined as achieved if the aircraft is within an imaginary sphere which surrounds the waypoint. This sphere could be elongated so that it resembles more of a cylinder so that only passing through the appropriate latitude and longitude would register the waypoint as achieved and request the new waypoint from the waypoint state machine. The plane should attempt to achieve the center of each predetermined waypoint.

5.5.4 Calculating required attitude to the next waypoint

The heading calculation required to get from the aircrafts current position to the next waypoint using great circle navigation is shown in appendix B.5.

This uses the latitude and longitude and altitude $lat1$, $lon1$ and $altitude1$ of the desired waypoint and the latitude, longitude and altitude $lat2$ and $lon2$ and $altitude2$ of the aircrafts current position to determine a distance and heading to the next waypoint. Granted this is overkill for the current state of the project.

5.5.5 Course corrections, adjusting for environmental effects

Course corrections between the Heading (measured by the magnetometer), the direction the aircraft is facing, and the Bearing, the direction of the aircrafts velocity relative to the earth (comes from GPS) gives the error in

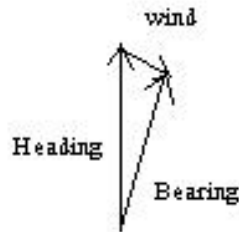


Figure 5.5: Wind can be calculated as the difference between heading and bearing

flight path due to wind. This wind vector can be calculated as the difference of the two vectors. As in figure 5.5.5.

5.6 Flight dynamics

5.6.1 Roll

The control system assumes that there is zero roll to be correct. This assumption is discussed here, and in the results section. This assumption is not true at all times, nor is it at all true for all airframes. So the effects which cause roll should be understood to know how to reduce the effect or to make sure that, and understand how the airframe will re-stabilize laterally (about the X axis).

The pendulum effect

A high wing configuration uses the pendulum effect to self-level the plane about the axis of roll. Of course this means that the lower the Center of Gravity (CG) is relative to the wing, the greater this roll moment will be, since the mass will provide a greater torque moment. While lowering the CG now appears to be beneficial the effect of a side gust of wind should be taken into account. If the Center of Pressure (CP) from the wind force is below the CG of the plane then the aircraft will roll to oppose the force. However if the CP is above the CG then the aircraft will roll to enforce the disturbing force. So the CG should be low to self level the wings but not too low that the airframe becomes unstable due to side wind forces.

Dihedral slip-roll coupling

In the presence of dihedral, a disturbance of uncoordinated (side-to-side) airflow causes an aircraft to roll away from its normal position, the aircraft will side slip in the direction of the down-going wing. This creates a lateral airflow component along the length of the wing. The dihedral angle can be seen as presenting a positive angle of attack to this lateral flow on the lower wing and a lower angle of attack on the higher wing, therefore providing a restoring torque which is proportional to the dihedral angle and proportional to the amount of slip. This returns the aircraft to its normal attitude. Preferably, due to the assumptions, to zero roll, if trimmed correctly. Also the fuselage shadowing one wing most notable on high-wing aircraft produces slip-roll coupling, swept wings produce slip-roll coupling, and a tall rudder that sticks up above the roll axis produces slip-roll coupling. The slip-roll coupling combines with the long-tail slip effect where there is a long tail present to give the airplane roll-wise stability.

Differential Wingtip Speed, Over Banking

When an aircraft is in a coordinated turn the outside wingtip follows a path of length $2 \pi R$, while the inside wingtip follows a smaller radius of $2 \pi r$. The outside wingtip must travel a greater distance in the same amount of time; therefore it has to move faster.

Since the lift generated by an airfoil depends on the square of the airspeed, the outside wing produces more lift. This causes the aircraft turning to tend to bank more and more into the turn, called over banking. The tighter the turn, the greater the velocity difference becomes which can lead to a spiral dive. To reduce over banking the ailerons should be deflected against the turn.

This effects torque depends on the ratio of the wingspan to the radius of turn. Short wings, high airspeed, and shallow bank angle, have less effect than long wings, low airspeeds and steep turns.

Propeller Drag Rolling Moment

The engine also contributes to the roll-wise torque budget. The propeller does not throw the air straight back. There is rotational drag on the propeller blades. Newtons law of action and reaction [11] says that if the prop throws the air down clockwise, it tends to make the airplane roll anticlockwise, as viewed from behind.

Some of the rotating air hits the top of the right and the bottom of the left wing and horizontal stabilizer. This reduces the amount of roll, but

not completely. Using Newton's law again, any air which escapes while still rotating clockwise, must torque the airplane anti-clockwise.

To counteract this effect a corresponding amount of air must be thrown down on the opposite side of the rotation. This can be achieved by setting the left wing at a slightly lower angle of incidence than the right wing, called asymmetric angle of incidence. The asymmetry should be in the part of the wing that flies in the prop-wash, so that the effect increases as engine power increases. Also the ailerons are used to counter the prop drag rolling moment.

Engine Inertia

Torque equals the rotational inertia times the rotational acceleration as from Newton [11]. So if engine revs are increasing or decreasing, a torque will be produced.

Due to conservation of momentum if a clockwise rotational momentum is given to an object, then a counter-clockwise rotational momentum was imparted on something else. So if the engine speed is changing, the airplane will tend to roll if the rotational momentum is not counteracted. This is worst in the case where the engine and propeller spin in the same direction. So using a gearbox would be preferable. Also if you change the orientation of the plane of rotation gyroscopic precession will cause moments about the other axis.

Discounting Roll

All the effects mentioned can be combined so that a high-wing, swept-wing airplane with lots of dihedral, a really high tail and a counter rotating prop would probably give more roll stability than is necessary.

A positively stable aircraft when disturbed from its trimmed flight state, will commence an initial movement back toward the trimmed flight state, but probably over-run it. If the oscillations are damped the aircraft is said to have dynamic stability. An aircraft which initially makes a movement back toward the normal flight state is called statically stable. The magnitude of the oscillation and the time for the oscillations to damp out gives the aircraft's response rate to instability. Unfortunately a statically stable aircraft can be dynamically unstable in that plane i.e. the oscillations do not damp out.

With slip-roll coupling a relatively normal turn can be performed using just the rudder. If you gently press on the right rudder, you will cause a skid that will eventually produce a bank to the right. If you hold a constant rudder deflection, the turning force will be proportional to the rudder deflection,

whereas the bank will keep getting larger and larger because of the slip-roll coupling.

If, for some reason, one wing goes a bit lower than the other so that some roll is incurred the airplane will begin to turn. If the turn were perfectly coordinated, the airplane would continue to turn around. Fortunately, this type of turn will be a slipping turn. The small amount of slip, acting through the slip-roll coupling, will tend to roll the airplane back to level flight about the roll axis. Provided that the un-commanded bank does not approach the limit where the over banking tendency tends to take over, the aircraft will remain stable in roll in the long term, provided the airframe is chosen appropriately.

Chapter 6

Airframe

The control system described in previous chapters can be used for any servo-controlled airframe. We chose the Grand Wing Servo-tech (GWS), E-Starter as the airframe for the first flight tests. A photo of the completed airframe is shown in Figure 1.1.

The Specifications for the test craft can be seen in table 6.1.

The airframe was chosen on the following parameters, according to the effects outlined in section 5.6.1:

- Large amount of dihedral.
- High tail plane.
- Long tail.
- Gear boxed engine and propeller for counter rotation.
- Light weight so that it can be electric powered removing the setup time required of petrol motors. This also renders the plane fairly harmless.
- Cheap, the airframe cost less than fifty NZ dollars.
- Low airspeed, so that visual range is maintained for a long amount of time, necessary for viewing the performance of the autopilot.
- maneuverability, the plane is capable of being put into extreme attitudes so that the autopilots recovery from such states can be assessed. Also if the auto pilot failed the remote pilot could recover control easily.
- The airframe is an ARF (Almost Ready to Fly) kit so no time would be spent on design. Also the kit can be assembled easily in a day.

- Polystyrene airframe meant that any damage could be fixed with some glue at the test site so that the plane could be ready quickly for another flight.

| | |
|-------------------|--|
| Make | Grand Wing Servo-tech (GWS) |
| Model | E-Starter |
| Total weight | 0.395 Kg |
| Length | 0.725 m |
| Wingspan | 0.960 m |
| Wing loading | 23 g/dm ² (7.6 oz/ft ²) |
| Max Airspeed | 20 kph |
| Cruising Airspeed | 15 kph |
| Engine | EPS-300C |
| Propeller | EP-1080 |
| Thrust | 0.332Kg (11.1 oz) |
| Power | 93 W |
| Efficiency | 3.57 g/W |
| Battery | 9.6V 750mAh Ni-MH |
| Flight Time | 20 minutes |
| Trailing antenna | none |

Table 6.1: GWS E-Starter airframe specifications

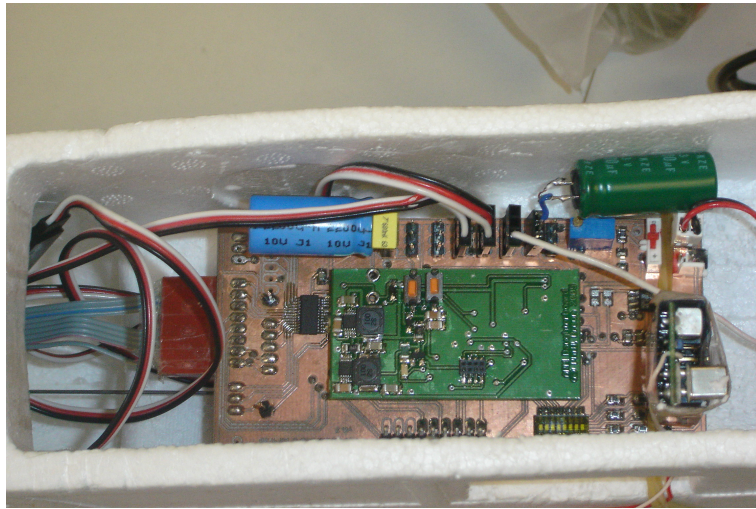


Figure 6.1: The control system installed onto the E-Starter

Chapter 7

Test Flight Results

Once the airframe was completed, the magnetic navigation system was ground-tested in the laboratory (see Section 7.5). The next step is to test the control system on a real flight.

7.1 Goals

The testing intends to achieve three things. Firstly to test the control systems ability to switch between autonomous mode and remotely piloted mode. Secondly to put the attitude control system through its paces to see how it responds to a different initial attitude as it attempts to command an attitude of its own. Thirdly, test the control systems performance in a variety of weather conditions. The flight time of the aircraft is approximately 20 minutes so the goals are broken down and attempted over various flights. These goals would be tested according to the following schedule:

- Ground test the control system, test the control system by moving the aircraft into various attitudes on the ground and see how it responds when the aircraft does roll, at the limits of the attitudes e.g. $\pm 90^\circ$ pitch, see if it looks right. Do the surfaces move in the correct direction in response to an error in attitude. Can the control system be reliably changed in and out of autonomous control.
- Flight test the autonomous mode switching
- When weather conditions are calm and dry, pilot the aircraft to an orientation which is close to the control systems desired (predetermined and hard coded by the user) value so that the error term is small and switch the aircraft into autonomous mode. Monitor whether level flight is maintained in the desired direction.

- Incrementally increase the initial heading error to 90 degrees over successive flights but maintain level flight so that the heading error is increased so the aircrafts ability to turn to the desired heading is tested.
- Set the aircraft to an initial pitch toward the sky (negative pitch) by a small amount while the heading is approximately the desired value
- Increase this pitch error to -45 degrees incrementally over successive flights.
- Set the aircraft to an initial pitch toward the ground (positive pitch) by a small amount while the heading is approximately the desired value
- Increase this pitch error to as much as possible by the airframe incrementally over successive flights.
- increase the initial heading error to greater than 90 degrees up to 180 degrees east and west over successive flights but maintain level flight so that the heading error is increased only then aircrafts ability to turn to the desired heading is tested.
- Mix the two attitudes so that the control system starts with an attitude error which is orientated in both the pitch and heading directions. Increasing the total rotation required by the control system to re-orientate the aircraft to the desired attitude.
- Test the control systems ability as per above in less than perfect weather conditions, such as Gusty or light rain conditions.

7.2 Method

Due to deadlines (the due date for this project was just over seven months from its conception), and small windows of low-wind weather at the time of year of the testing (spring), it was important to be very productive when conditions were favorable.

Testing required the help from several people, including camera people and a pilot, at a time of year which most students are very busy. Again, adding to the necessity for being productive during testing. Thus the following methodology was used:

- Perform the calibration for the airframe
- Trim airframe with control system on-board

- Select a site for the flight
- Set clear goals for each test
- Build on results when successful to increase difficulty for control system
- Record results using video footage from the ground

The implementation of this plan is laid out in the following sections.

7.3 Trimming, Balancing and calibrating the airframe

The calibration was performed as outlined in section 5.1.3 for each of the magnetometer axis. The gains and offsets calculated where:

- X-axis: Offset = 2140, Gain = 1.21
- Y-axis: Offset = 1854, Gain = 1
- Z-axis: Offset = 2223, Gain = 1.2

The control surfaces were then trimmed for zero deflection when the control system commanded an angle of zero deflection. The Aircraft was then balanced on the ground approximately then flown via remote control with the flight system fitted to test for the correct balance. The CG was found to be too far back due to the magnetometer board located in the far end of the tail. The battery pack was moved forward to account for this and the plane retested. This showed it to be successfully balanced. During this successful balancing test flight the pilot trimmed the aircraft for level flight at 3/4 throttle.

7.4 Select a location

The location selected was the Dunedin Model Aero Club grounds at School Rd, Mosgiel. This site was selected because it is known to be airspace occupied by model sized aircraft and is in a rural area where radio interference would be unlikely on the frequency used for the remote pilot control (36.090 MHz). Selecting some co-ordinates at regular intervals within 20km of the site and inputting the co-ordinates into the IGRF's (International Geomagnetic Reference Field) model shows that the magnetic field is fairly stable around the location:

The test site had the following parameters:

| Location | Aero club | Mosgiel town | Caversham hill |
|---------------------------|--------------------------------------|---------------------------|---------------------------|
| GPS Co-ordinates | S 45deg 52.17293' E 170 15.90454' | S 45 53.29 E 170 21.48 | S 45 53.29 E 170 28.29 |
| Altitude HAE | 12.1m | 10.0m | 30.0m |
| Date | 2005.6191 | 2005.6191 | 2005.6191 |
| Declination | 24.434° | 24.453° | 24.466° |
| Inclination | -70.57° | -70.566° | -70.552° |
| X component (nT) | 17,789.55 | 17,788.33 | 17,794.18 |
| Y component (nT) | 8,082.39 | 8,088.99 | 8,096.38 |
| Z component (nT) | -55,394.1 | -55,384.95 | -55,366.62 |
| Horizontal intensity (nT) | 19,539.53 | 19,541.15 | 19,549.53 |
| Total intensity (nT) | 58,739.25 | 58,731.16 | 58,716.66 |

Table 7.1: Magnetic field information near Dunedin

- GPS location: S 45deg 52.17293', E 170 15.90454'
- Magnetic field vector: X component = 17,789.55 nT, Y component = 8,082.39 nT, Z component = -55,394.1 nT
- Type of airspace: NOTAM'd (NOTice To AirMen) as model aero club space, where model aircraft are likely. The airspace is also used for low level flight training operations by Mainland Aviation College, Massey University School of Aviation, and Otago Aero Club.
- Time of flights: Between 5pm and 7pm due to the pilots working hours.
- Altitude (HAE (height above ellipsoid)): 12.1m
- Weather conditions: Variable, inland several kilometers so tends to measure lower airspeeds and the location being near the Dunedin airport meant that updated weather information such as wind-speed and rainfall where readily available.
- Terrain and visibility: Surrounded by small hills with a large flat plain about 5km in radius of rural paddocks and low in altitude meant that provided the weather conditions were favorable the visibility would be likely to be very large and cloud base would be a decent distance above the intended operating altitudes.

7.5 Results

Day one (27/9/05): The aim on day one was to perform the calibration steps and to balance and trim the airframe. Alan Coppard kindly volunteered to act as our test pilot. Alan is a highly skilled RC pilot.

- Calibration, performed for magnetometers as per section 5.1.3. The values were updated on location using a laptop set up as pictured in 7.1.
- Trim, This was set for the remote pilots controller so that the autonomous mode is switched on when the transmitters fourth channel control lever is centered. Also the elevator and rudder trim was adjusted so that with the controls centered and 3/4 throttle the aircraft would maintain level flight.
- Throttle. The throttle required to fly the aircraft at a reasonably low angle of attack of around 5 degrees was found to be about 3/4 throttle. So the control systems commanded throttle for the test flights was increased from 1/2 to 3/4 throttle.
- Weight, the center of gravity (CG) was found to be too far back. The battery pack was moved further forward to compensate for the magnetometer sensors being located at the far end of the long tail (near the rudder).
- Duration of flight, 10 minutes

Day two (29/9/05):

- Trim, The Magnetometer board was rotated in pitch so that the elevator attempted to hold a small amount of pitch while the plane was held level on the ground. When the system was engaged into autopilot in the air the aircraft remained relatively level but the angle of attack was not sufficient for the constant airspeed selected. So the magnetometer board was rotated on its mount slightly, which involves unpinning the polystyrene block which it is mounted on and re-pinning the block after pitching the magnetometer board down.
- The throttle was decided to be still slightly low also so this was increased to 80 percent.
- Weight adjustment seemed to have been successful.

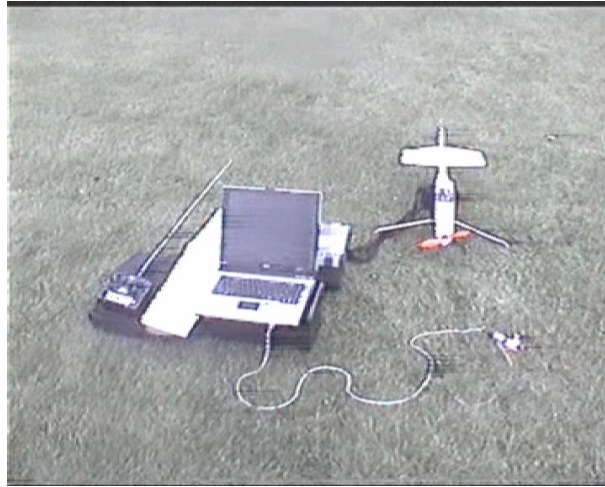


Figure 7.1: The ground station setup for updating the firmware, offsets, and gains in the field

- Successful changing between modes while airborne (RPV/Autonomous)
- Successful heading hold, attitude stabilization
- Successful turn toward desired heading (north from west) approximately 20 degrees to start with then increased over three attempts to approximately 90 degrees. Stable, level flight in the correct heading was quickly regained in approximately 5 seconds from 90 degrees heading error. See photo sequence below.
- Successful remote control takeoff and landings. The pilot and airframe have at this point successfully completed several takeoff and landings while under remote pilot control.
- Successful footage of testing was taken, There is a need for lower flight and more tests to be able to assess oscillation, from current footage plane seems to be excellent with plenty of airframe damping. Even in slight gusts of approximately 10kmh which is comparable to the aircrafts 20kmh airspeed, which can be seen in the video footage.
- The biggest problem for the testing is the poor range of the R/C transmitter which is quoted to 1.5km but only achieves a maximum of less than 50m. This range is far too small, the plane becomes uncontrollable by the remote pilot outside of this range and the safety feature implemented in this version of the flight controller causes the aircraft

to default into remote control which is just noise picked up by the receiver so the plane loses control and turns off its throttle causing the aircraft to crash. This range needed to be increased in order to fully assess the control system over a longer duration.

- Duration of flight 20 minutes

Day three (2/10/05):

- The range problem necessitated the change of the radio equipment. This involved swapping the receiver which plugs into the main board and using a different higher powered transmitter. This was an opportunity to see how the system would cope with the change in equipment, assessing its ability to work with off the shelf radio control components. The result was a success and the range was increased to over 1km even though the transmitters battery was less than completely full so flight testing could commence.
- Hand launching the aircraft was successful and footage was obtained so that an algorithm can be developed to remove the pilot needing to initially take off the aircraft.
- The control system was now ready to try and recover the aircraft from first a climb and then a dive attitude. The aircraft was faced north and put into a climb of approximately 20 degrees and then switched into autonomous mode. The correct attitude of wings level and flying North was achieved within two seconds of being engaged. So a dive was attempted. Shallow to start with, only 20 degrees down, and this was also recovered within two seconds. So the plane was climbed to a safe altitude once again and dived toward the ground at approximately 45 degrees from which it recovered in approximately 3 seconds as seen in the video footage of the introduction clip. The control system has not yet implemented the designed airspeed sensor so there is no feedback for the velocity of the aircraft. This causes an oscillation in pitch recovering from the dive where airspeed has been increased since as discussed earlier the amount of control required to change the aircrafts state varies with air speed. This oscillation would be dampened out if the integral and proportional parts (as per section 5.4.1) of the PID were implemented. This effect was not really found to increase at steeper pitch angles due to the slow terminal velocity of the airframe.
- Now it was time to test the control systems ability to adjust the heading for errors greater than 90 degrees. The aircraft was flown south

west when the on-board controller was requesting level north flight and then autonomous mode was selected. The aircraft was known from ground testing that it would attempt some sort of wing over maneuver to attempt to rotate to the desired attitude. The control input seemed to be satisfactory; a little aggressive but for the chosen airframe is a valid maneuver. At larger heading errors however, closer to 180 degrees the current control system attempts to smoothly put less control into the rudder so that the transition from a left or right turn by the rudder is smooth. This is necessary since at 180 degrees error the control system would request maximum rudder left or right other wise. Often rapidly flicking between both, until a small rotation away from this case is achieved. Commanding the servos in this way causes them to drain a large amount of current and could have caused the control system to reset due to low voltages, caused by the internal resistance of the batteries and speed controller not being able to supply the required current. So the rotation requested at exactly 180 degrees heading is a pitch upwards. This pitch upwards caused the aircraft to stall since the throttle is not actively adjusted and the aircraft yaws to the left or right. The change in heading sufficiently calculates a rotation for the heading about the z axis and commands increasing amounts of rudder. This process looks like a messed up wing over but does successfully bring the plane around to the desired heading with wings level without losing any height. It is a rare situation for the control system to be flying 180 degrees away from the desired direction of travel but this situation could occur if a waypoint was requested of the current control system which was directly behind the aircrafts current direction of flight. So it was necessary to test.

- It was time to test the planes response to an arbitrary initial attitude state and record its response to attempt to fly the aircraft wings level and heading North. The response of the control system about the combined y and z axis was the same as the aircrafts response about each of the axis individually. Pitch rotations about the y axis were more responsive than heading rotations about the z axis as would be expected.
- The control system has received a variety of wind and rain conditions over span of the testing period. It's response to gusts tends to be a translational slip as the system manages to maintain the heading and pitch directions relatively stably. The aircraft can be seen flying in light rain successfully in the footage of this day's (day 3) testing



Figure 7.2: A series of still images from video footage showing the transition from pilot control to autonomous control. The frames read from left to right, top to bottom. They are taken at regular intervals every 18 frames which represents approximately 0.71s depicting a controlled turn toward north.

without much difficulty. This means that a flight does not necessarily need to be aborted due to rain which is advantageous.

- Total duration of flights, 60 minutes. Total flights on the day, 4

Chapter 8

Conclusions

Apeliotes has been successful in magnetometer based attitude control. The control system successfully regained control to level flight with the desired heading (geographical North). A pilot on the ground commanded various initial orientations of pitch and heading from which the control system had to recover. The first autonomous flight was achieved on 29/9/05, seven months after the projects conception. A GWS E-Starter model aircraft was fitted with standard low cost radio control hobbyist equipment and the Apeliotes autonomous flight controller.

As described in this paper, the controller used only a three axis magnetometer sensor to determine an attitude solution in pitch and heading with the assumption of zero roll. This assumption proved to be valid for the control system as the a roll motion turned out to couple through the measurements in such a way that the system remained stable at all attitudes including rolls so that the plane attempts to zero the roll using control itself. In a knife edge position the aircraft will attempt to yaw the plane so that it is nose up where the system can now apply elevator to force the pitch to zero so that the wings are now level. If upside down, the control system attempts to loop back to the desired attitude. So the zero roll assumption does not cause the aircraft to loose control when there is roll present.

On the third day of testing the longest and most difficult flight of the testing session was accomplished. The aircraft was initially put in a dive of 45 degrees toward the ground at an altitude of 20m above the ground heading 90 degrees off north. The control system successfully regained control and turned to make the required rotation of yaw and pitch to fly in the requested direction of geographic north for a distance of approximately 100m before being switched back out of autonomous mode to continue testing.

A solution seems to be possible about the roll axis by using more magnetometers but this will need to be investigated further. Along with numerous

upgrades some of which are listed below, in the Section labeled further work.

8.1 Further work

This project is very extensible. The functionality which follows is intended to be implemented into Apeliotes in the future. These could be adopted by anyone for research.

8.1.1 Coping with noise and inaccuracy

Noise and inaccuracy is introduced at many stages such as the sensors, amplification, sampling, data storage and processing etc. These sources of noise can be overcome using filtering and appropriate choices of units to represent numbers.

- Hardware filtering: Butterworth filtering, active filtering, digital links.
- Software Filtering: Kalman Filtering. Extended Kalman filtering

8.1.2 Number representation

an attempt has been taken to represent numbers with units so as to produce a value close to one. This reduces inaccuracies introduced from overflow and underflow during mathematical computations. More time should be taken to further implement this throughout the code to increase accuracy now that the initial code has proved to work. Any further work should maintain this policy.

8.1.3 Further development

- Long range telemetry
- 3D Simulator port
- HUD GUI from telemetry
- Topographical Flight planning interface
- Higher order control: having completed the first order approach successfully it is time to consider higher order control utilizing the available information....
- Altitude hold: Controlling Rate of Climb, Controlling Altitude

- simple take-off: button on side revs engine to max rpm then level throw in direction letting go initializes level climb to some altitude when it switches into flight plan to do waypoints...
- maintaining optimum airspeed: feedback of airspeed measurement.....
- Optimized turning: using accelerometers for turn coordinating.... gyros.....
- Simple landing: engine throttle decrease with level decent, path given by input waypoints....

Appendix A

Quaternions

Quaternions are a vector containing 4 scalar variables; quaternions can be added and multiplied as a normal number. There is however a difference, unlike the algebra of scalar numbers quaternion multiplication is not commutative. Quaternions have 4 dimensions with 4 variables. One dimension is real and the other 3 are imaginary dimensions. Each of the imaginary dimensions has a unit value equal to the square root of -1, but are different square roots of -1, each mutually perpendicular to each other, denoted as i , j and k . Since quaternions work in 4 dimensions there are at least 3 ways to get from +1 to -1. Quaternions take the form $Q = a + ib + jc + kd$.

Quaternions are useful for representing rotations in three dimensions (3D). To do this the quaternions are normalized so that they have unit magnitude. Once normalized, multiplications are used to represent a combination of different rotations once normalized.

Quaternions used in this way can be thought of as being similar to axis-angles except that the real part is equal to $\cos(\frac{\omega}{2})$ (where ω is the angle of rotation) and the complex parts are made up of the axis vector times $\sin(\frac{\omega}{2})$. The angular representation of the quaternion is,

$$q = \cos\left(\frac{\omega}{2}\right) + i(x * \sin\left(\frac{\omega}{2}\right)) + j(y * \sin\left(\frac{\omega}{2}\right)) + k(z * \sin\left(\frac{\omega}{2}\right))$$

where ω is the angle of rotation and x , y , and z represent the components of the vector about which the rotation occurs. So quaternions are closely related to the axis-angle representation of rotations.

The quaternion i represents a rotation of 180 degrees about the x-axis, the quaternion j represents a rotation of 180 degrees about the y-axis, and the quaternion k represents a rotation of 180 degrees about the z-axis. So $i * i = -1$ represents a rotation of 360 degrees about the x-axis.

The negative of a quaternion represents the same rotation. So if $(w + xi + yj + zk)$ represents a rotation then $(-w - xi - yj - zk)$ represents the

same rotation although it is a different quaternion. The rotation is the same because the angle is reversed but also the axis is reversed.

Quaternions are spinors. An object which, if rotated by 360 degrees is inverted, is known as a spinor. Spinors provide a means of representing rotations in n dimensions. They were first defined by physicists working in the field of quantum mechanics. Spinors in four-dimensional space occur in Dirac's equations for the wave functions of an electron.

A.1 Multiplying quaternion numbers

The multiplication rules for quaternions are:

$$\begin{aligned}
 i \times i &= j \times j = k \times k = -1 \\
 i \times j &= k \\
 j \times i &= -k \\
 j \times k &= i \\
 k \times j &= -i \\
 k \times i &= j \\
 i \times k &= -j
 \end{aligned}$$

Where quaternion 1, $z1 = (a + ib + jc + kd)$ and quaternion 2, $z2 = (e + if + jg + kh)$

The multiplication of quaternions expands as follows:

$$\begin{aligned}
 &(a + ib + jc + kd) \times (e + if + jg + kh) \\
 = & \\
 &a(e + if + jg + kh) \\
 &+ ib(e + if + jg + kh) \\
 &+ jc(e + if + jg + kh) \\
 &+ kd(e + if + jg + kh) \\
 = & \\
 &a \times e + ia \times f + ja \times g + ka \times h \\
 &+ ib \times e + i \times i \times b \times f + i \times j \times b \times g + i \times k \times b \times h \\
 &+ jc \times e + j \times i \times c \times f + j \times j \times c \times g + j \times k \times c \times h \\
 &+ kd \times e + k \times i \times d \times f + k \times j \times d \times g + k \times k \times d \times h \\
 = &
 \end{aligned}$$

$$\begin{aligned}
& a \times e + ia \times f + ja \times g + ka \times h \\
& + ib \times e - b \times f + k \times b \times g - j \times b \times h \\
& + jc \times e - k \times c \times f - c \times g + i \times c \times h \\
& + kd \times e + j \times d \times f - i \times d \times g - d \times h
\end{aligned}$$

=

$$\begin{aligned}
& a \times e - b \times f - c \times g - d \times h \\
& + i(b \times e + a \times f + c \times h - d \times g) \\
& + j(a \times g - b \times h + c \times e + d \times f) \\
& + k(a \times h + b \times g - c \times f + d \times e)
\end{aligned}$$

The result is:

$$\begin{aligned}
z1 \times z2 = & \\
& a \times e - b \times f - c \times g - d \times h + \\
& i(b \times e + a \times f + c \times h - d \times g) + \\
& j(a \times g - b \times h + c \times e + d \times f) + \\
& k(a \times h + b \times g - c \times f + d \times e)
\end{aligned}$$

Appendix B

Significant code

The following code is written in C. It shows some excerpts from the most significant parts of the control system. The Fixed16 declaration is part of a complete fixed point math library. The format for a Fixed16 number here is 16.16 bits.

B.1 Reference field rotation

```
Fixed16 qr0 = cos(m_roll/2)*cos(m_pitch/2)*cos(m_yaw/2) + sin(m_roll/2)*sin(m_pitch/2)*sin(m_yaw/2);
Fixed16 qr1 = sin(m_roll/2)*sin(m_pitch/2)*cos(m_yaw/2) - cos(m_roll/2)*sin(m_pitch/2)*cos(m_yaw/2);
Fixed16 qr2 = cos(m_roll/2)*sin(m_pitch/2)*cos(m_yaw/2) + sin(m_roll/2)*cos(m_pitch/2)*sin(m_yaw/2);
Fixed16 qr3 = cos(m_roll/2)*cos(m_pitch/2)*sin(m_yaw/2) - sin(m_roll/2)*sin(m_pitch/2)*cos(m_yaw/2);

Fixed16 two(2);

Fixed16 x_field = qr0*qr0>trueN_field.x + two*qr2*qr0>trueN_field.z - two*qr3*qr0>trueN_field.y +
qr1*qr1>trueN_field.x + two*qr2*qr1>trueN_field.y + two*qr3*qr1>trueN_field.z -
qr3*qr3>trueN_field.x - qr2*qr2>trueN_field.x;

Fixed16 y_field = two*qr1*qr2>trueN_field.x + qr2*qr2>trueN_field.y + two*qr3*qr2>trueN_field.z +
two*qr0*qr3>trueN_field.x - qr3*qr3>trueN_field.y + qr0*qr0>trueN_field.y -
two*qr1*qr0>trueN_field.z - qr1*qr1>trueN_field.y;

Fixed16 z_field = two*qr1*qr3>trueN_field.x + two*qr2*qr3>trueN_field.y + qr3*qr3>trueN_field.z -
two*qr0*qr2>trueN_field.x - qr2*qr2>trueN_field.z + two*qr0*qr1>trueN_field.y -
qr1*qr1>trueN_field.z + qr0*qr0>trueN_field.z;

//set the global variables
vars->x_vect = x_field;
vars->y_vect = y_field;
vars->z_vect = z_field;
```

B.2 Map measured field to reference field

```
Fixed16 q0 = -trueN_field.x*observed_field.x - trueN_field.y*observed_field.y- trueN_field.z*observed_field.z;
Fixed16 q1 = trueN_field.y*observed_field.z - trueN_field.z*observed_field.y;
Fixed16 q2 = -trueN_field.x*observed_field.z + trueN_field.z*observed_field.x;
Fixed16 q3 = trueN_field.x*observed_field.y - trueN_field.y*observed_field.x;
```

B.3 Rotation from measured to reference magnetic field for attitude

```
Fixed16 q0 = -trueN_field.x*observed_field.x - trueN_field.y*observed_field.y - trueN_field.z*observed_field.z;
Fixed16 q1 = trueN_field.y*observed_field.z - trueN_field.z*observed_field.y;
Fixed16 q2 = -trueN_field.x*observed_field.z + trueN_field.z*observed_field.x;
Fixed16 q3 = trueN_field.x*observed_field.y - trueN_field.y*observed_field.x;
```

B.4 Proportional control

```
inline FixedVector calc_control()
{
    Fixed16 pitch_gain(Fixed16(2));
    Fixed16 yaw_gain(Fixed16(7));

    Fixed16 roll_error(vars->roll_vect); // radians
    Fixed16 pitch_error(vars->pitch_vect); // radians
    Fixed16 yaw_error(vars->yaw_vect); // radians

    //NED reference frame with the right hand rule for rotations
    Fixed16 set_aileron = Fixed16(45);
    Fixed16 set_elevator = Fixed16(-((pitch_error*pitch_gain*2*45) / pi) + 45);
    Fixed16 set_rudder = Fixed16(((yaw_error*yaw_gain*45) / pi) + 45);

    return FixedVector(set_aileron, set_elevator, set_rudder);
}
```

B.5 Navigation

```
fixed32 GC_distance(fixed32(lat1), fixed32(lon1), fixed32(lat2), fixed32(lon2), fixed32(altitude))
{
    fixed32(radian_dist);
    fixed32(earths_radius) = 6366710;

    //radian distance on the earths surface.
    return 2*asin(sqrt((sin((lat1-lat2)/2))^2 + cos(lat1)*cos(lat2)*(sin((lon1-lon2)/2))^2));

    //distance in meters
    //return (altitude + earths_radius) * radian_dist;
}

fixed32 DMS_to_rad(fixed32(degrees), fixed32(minutes), fixed32(seconds))
{
    return (degrees + minutes/60 + seconds/3600)*(Fixed16::PI())/180;
}

//however this is NW positive signs
fixed32() true_course(fixed32(lat1), fixed32(lon1), fixed32(lat2), fixed32(lon2), fixed32(altitude))
{
    fixed(d) = GC_distance(lat1, lon1, lat2, lon2, altitude);

    //special case of starting at the poles
    if(cos(lat1) < EPS){ // EPS a small number ~ machine precision
        if(lat1 > 0)
            return (Fixed16::PI()); // starting from N pole
        else
            return 2*(Fixed16::PI()); // starting from S pole
    } else {

    //For starting points other than the poles:
    if( sin(lon2-lon1)<0)
        return acos((sin(lat2)-sin(lat1)*cos(d))/(sin(d)*cos(lat1)));
    else
        return (2*pi-acos((sin(lat2)-sin(lat1)*cos(d))/(sin(d)*cos(lat1))));

    // //alternative formula not requiring the computation the distance between the points is:
```

```

// return mod(atan2(sin(lon1-lon2)*cos(lat2),
//             cos(lat1)*sin(lat2)-sin(lat1)*cos(lat2)*cos(lon1-lon2)), 2*pi);
}
}

void init_navigation(void){
struct uav_vars* vars = VAR_ADDR;

vars->waypoint_ptr = 0; //next waypoint to achieve is at position 0 in the waypoint array

//-----waypoints-----
//first waypoint:
vars->waypoints[0][0] = 0; //latitude (radians)
vars->waypoints[1][0] = DMS_to_rad(170, 15.90454, 0); //longitude (radians)
vars->waypoints[2][0] = 30.1; //altitude HAE (m)

//-----

vars->GPS_ptr = 0;
}

```

Bibliography

- [1] NOVA Boston public television station. Spies that fly. VHS, January 7, 2003.
- [2] Phill Brown. An efficient compact, gps-enabled 32-bit control module. In *Proceedings of ENZCON*, 2004.
- [3] Donald E. Catlin. *Estimation, Control, and the Discrete Kalman Filter*. Springer, 1 edition, November 9, 1988.
- [4] S. Chapman and J. Bartels. *Geomagnetism*. Oxford Un. Press Ed., 1940.
- [5] John S. Denker. *See how it flys*. av8n, 2005.
- [6] Simon Harvey. 3 dimensional model of the e starter airframe. 3D mesh and textures, 2005.
- [7] Jack B. Kuipers. *Quaternions & Rotation Sequences, A Primer with Applications to Orbits, Aerospace, and Virtual Reality*. Princeton University Press, 2002.
- [8] TRIMBLE Navigation ltd. Lassen sq gps module specifications. Technical report, TRIMBLE Navigation ltd, 2004.
- [9] MAXIM. Max1227/max1229/max1231 user manual. Technical report, MAXIM Integrated Products, July 2003.
- [10] Tatiana Bondar Vadim Golovkov Benoit Langlais Frank Lowes Nils Olsen John Quinn Terry Sabaka Mioara Manda, Susan Macmillan. International geomagnetic reference field. Technical report, International Association of Geomagnetism and Aeronomy (IAGA), January 2000.
- [11] Sir Isaac Newton. *Philosophiae Naturalis Principia Mathematica*. Cambridge, Trinity College, 2 edition, 1686.

- [12] The International Association of Geomagnetism and Aeronomy (IAGA). Us/uk world magnetic model for the epoch 2005, main field declination (d). webpage, December 2004.
- [13] N. W. Peddie. *International Geomagnetic Reference Field: The Third Generation*. J. Geomag. Geoelectr., 1985.
- [14] Rieker. Manual inclinometer: Model 2056e. web page.
- [15] Phillips Semiconductors. Lpc2119/lpc2129/lpc2194/lpc2292/lpc2294 user manual. Technical report, Phillips Semiconductors, 3 May 2004.
- [16] Phillips Semiconductors. Hef4017b msi 5-stage johnson counter user manual. Technical report, Phillips Semiconductors, January 1995.
- [17] Randall W Smith. *Department of Defense World Geodetic System 1984: Its definition and relationships with local geodetic systems*. Defense Mapping Agency, January 1991.
- [18] Wikipedia The free encyclopedia. Right hand rule. webpage, 2005. http://en.wikipedia.org/wiki/Right_hand_rule.